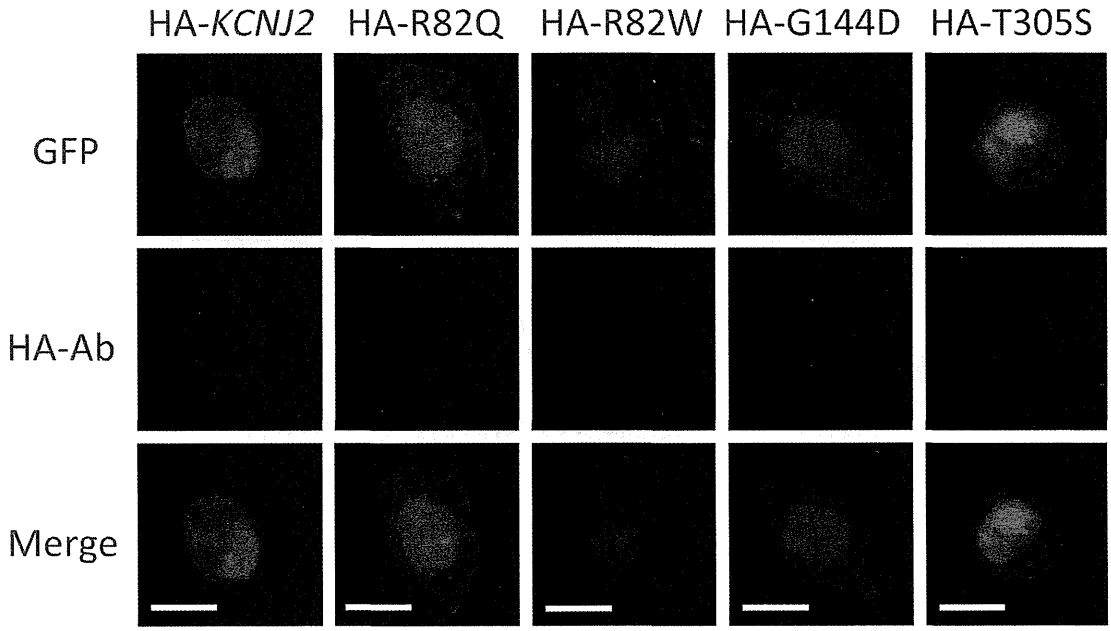

Figure 5. Cellular localization of wild-type (WT) and 4 mutant (R82Q, R82W, G144D, T305S) Kir2.1 channels. Hemagglutinin (HA)-*KCNJ2* indicates HA-tagged *KCNJ2* (positive control). **Upper panel** shows the green fluorescence of GFP; **middle panel**, red fluorescence of secondary anti-HA antibody; **lower panel**, merging of green and red fluorescences; **white bars** in the **merged panel** indicate 10 μm.

arrhythmias after the age of 10 years, and arrhythmias were reduced during pregnancy and after age 55 years, coinciding with menopause. In contrast, male mutation-positive subjects from the same family showed no ventricular arrhythmias but periodic paralysis. Interestingly, a case with R67W in our cohort was a male and complained of only periodic paralysis, supporting their conclusion, although there is a conflicting report by Donaldson et al.[26] They reported that the R67W mutation is capable of causing all phenotypes of ATS, and the pattern observed in the sex-specific kindred is not universal. It appears that other genetic or environmental factors contribute to a family's susceptibility to disease symptoms.

The topological location of *KCNJ2* mutations may influence the expression of ATS features. In the present study, C-terminal mutations were more frequent in the typical ATS group (Table 3). Zhang et al[14] also reported that dysmorphism and periodic paralysis were more frequently observed in C-terminal mutation carriers. The Kir 2.1 C-terminus relates to various types of loss of function in I_{K1} currents. Lopes et al[31] identified 12 basic residues in Kir2.1 that changed channel-PIP_2 interactions—10 of them were located in the C-terminus. The C-terminus also contains the endoplasmic reticulum (ER) export sequence, FCYENE, and the trafficking-related acidic cluster EEDDSE at positions 374 to 379 and 386 to 391, respectively.[32,33] More recently, we reported an S369X mutation located close to this ER export signal that impedes ER-Golgi transport.[7]

We tested the trafficking function of four mutations, and only G144D mutation showed a trafficking defect (Figure 5). Our results suggest that the phenotype expression variability of *KCNJ2* mutations may be influenced by the topological location of mutations; however, the other possibilities, for example, environmental factors, modifier genes, or SNPs,[34] remain unstudied.

Phenotypic Overlap Between CPVT and ATS

The prevalence of *KCNJ2* mutation carriers in the CPVT phenotype was lower than in the other phenotypes (Figure 1 and Table 1). Our 2 CPVT probands with *KCNJ2* mutation (G144D, T305S) had first syncope after the age of 30 years, and their ECGs showed bidirectional VT or PVCs at rest as well. In contrast, the age at first syncope of *RyR2*-related CPVT patients was reportedly younger age (mean age of 8 years),[10] and their syncope occurred mainly during exercise but not while resting. These findings, for example, late onset of symptoms and ventricular arrhythmia at rest, may be clues to distinguish between *KCNJ2*-related and *RyR2*- or *CASQ2*-related CPVT. Functional assays revealed that both G144D and T305S exerted dominant negative suppression effects on outward currents when coexpressed with WT Kir2.1 subunits. Apparently, therefore, baseline functional modulation by these mutations was not related to the phenotypic expression of ATS or CPVT.

Recently, a V227F mutation was identified in a patient with the typical CPVT phenotype but without dysmorphism or periodic paralysis.[35] A biophysical assay showed that heterozygous WT/V227F channels were identical to WT channels in function, but stimulation by cAMP-dependent protein kinase A (PKA) significantly downregulated the heterozygous mutant but not WT Kir2.1 currents. This particular type of loss-of-function may explain why the proband displayed the CPVT phenotype. More recently, Barajas-Martinez et al[36] demonstrated the characteristics of their patient with R260P mutation. She showed typical phenotypes of both ATS and CPVT. The β-blocker nadolol

was first used but ineffective. Her symptoms subsided after treatment with flecainide. She had dysmorphic features and bidirectional VT both at rest and during exercise testing. Functional analysis revealed that R260P mutation had strong dominant negative suppression effects, like that in our G144D case. Regarding our mutations, their modulation by PKA was not examined because they showed a significant loss-of-function at the baseline (Figure 4).

Phenotype and Channel Function

Although R82W, R82Q, G144D, and T305S were found in patients with an atypical phenotype of ATS (group B), these mutations showed dominant negative suppression effects on outward currents (Figure 4). Therefore, the results obtained for a heterologous expression system did not necessarily correlate with the clinical ATS severity. In this regard, Eckhardt et al[27] identified 4 *KCNJ2* mutations—R67Q, R82W, T75 mol/L, and T305A—in probands lacking the ATS triad and a family history of ATS. Surprisingly, we also identified R67W, R82W/Q, and T305S in group B. Therefore, residues of R67, R82, and T305 may be associated with atypical ATS phenotypes.

Study Limitations

Regarding CPVT probands, we screened 34 hot-spot exons of the *RyR2* gene. We could not exclude some variants in the remaining exons of *RyR2*. In conclusion, *KCNJ2* gene screening in patients with atypical ATS (only 1 of the ATS features or CPVT) phenotypes is of clinical importance, because 53% of mutation carriers were found to express atypical phenotypes, despite their severity of arrhythmia.

Acknowledgments

We are grateful to Dr Hitoshi Horigome, University of Tsukuba; Dr Norito Kokubun, Dokkyo Medical University; Dr Nobuyuki Murakoshi, University of Tsukuba; Dr Ichiro Niimura, Niimura Clinic; Dr Yuji Okuyama, Osaka University Graduate School of Medicine; Dr Takahiro Sato, Kanto Medical Center NTT East Corporation; Dr Yoshiaki Takahashi, Takahashi Pediatric and Cardiac Clinic; Dr Jun Yoshimoto, Shizuoka Children's Hospital; and Dr Masao Yoshinaga, National Hospital Organization Kagoshima Medical Center, for the contribution to this survey. We thank Arisa Ikeda for excellent technical assistance.

Sources of Funding

This work was supported by research grants from the Ministry of Education, Culture, Science, and Technology of Japan (to Dr Horie); National Natural Science Foundation of China (No. 30930105 to Dr Zhou and No 81170176 to Dr Zang); and health science research grants from the Ministry of Health, Labor, and Welfare of Japan for Clinical Research on Measures for Intractable Diseases (to Dr Horie).

Disclosures

None.

References

1. Andersen ED, Krasilnikoff PA, Overvad H. Intermittent muscular weakness, extrasystoles, and multiple developmental anomalies: a new syndrome? *Acta Paediatr Scand.* 1971;60:559–564.
2. Tawil R, Ptacek LJ, Pavlakis SG, DeVivo DC, Penn AS, Ozdemir C, et al. Andersen's syndrome: potassium-sensitive periodic paralysis, ventricular ectopy, and dysmorphic features. *Ann Neurol.* 1994;35:326–330.
3. Zaritsky JJ, Eckman DM, Wellman GC, Nelson MT, Schwarz TL. Targeted disruption of Kir2.1 and Kir2.2 genes reveals the essential role of the inwardly rectifying K(+) current in K(+)-mediated vasodilation. *Circ Res.* 2000;87:160–166.
4. Plaster NM, Tawil R, Tristani-Firouzi M, Canun S, Bendahhou S, Tsunoda A, et al. Mutations in Kir2.1 cause the developmental and episodic electrical phenotypes of Andersen's syndrome. *Cell.* 2001;105:511–519.
5. Ai T, Fujiwara Y, Tsuji K, Otani H, Nakano S, Kubo Y, et al. Novel *KCNJ2* mutation in familial periodic paralysis with ventricular dysrhythmia. *Circulation.* 2002;105:2592–2594.
6. Kobori A, Sarai N, Shimizu W, Nakamura Y, Murakami Y, Makiyama T, et al. Additional gene variants reduce effectiveness of beta-blockers in the LQT1 form of long QT syndrome. *J Cardiovasc Electrophysiol.* 2004;15:190–199.
7. Doi T, Makiyama T, Morimoto T, Haruna Y, Tsuji K, Ohno S, et al. A novel *KCNJ2* nonsense mutation, S369X, impedes trafficking and causes a limited form of Andersen-Tawil syndrome. *Circ Cardiovasc Genet.* 2011;4:253–260.
8. Haruna Y, Kobori A, Makiyama T, Yoshida H, Akao M, Doi T, et al. Genotype-phenotype correlations of *KCNJ2* mutations in Japanese patients with Andersen-Tawil syndrome. *Hum Mutat.* 2007;28:208.
9. Tester DJ, Arya P, Will M, Haglund CM, Farley AL, Makielski JC, et al. Genotypic heterogeneity and phenotypic mimicry among unrelated patients referred for catecholaminergic polymorphic ventricular tachycardia genetic testing. *Heart Rhythm.* 2006;3:800–805.
10. Priori SG, Napolitano C, Memmi M, Colombi B, Drago F, Gasparini M, et al. Clinical and molecular characterization of patients with catecholaminergic polymorphic ventricular tachycardia. *Circulation.* 2002;106:69–74.
11. McManis PG, Lambert EH, Daube JR. The exercise test in periodic paralysis. *Muscle Nerve.* 1986;9:704–710.
12. Tristani-Firouzi M, Jensen JL, Donaldson MR, Sansone V, Meola G, Hahn A, et al. Functional and clinical characterization of *KCNJ2* mutations associated with LQT7 (Andersen syndrome). *J Clin Invest.* 2002;110:381–388.
13. Bazett HC. An analysis of the time relations of electro-cardiograms. *Heart.* 1920;7:353–367.
14. Zhang L, Benson DW, Tristani-Firouzi M, Ptacek LJ, Tawil R, Schwartz PJ, et al. Electrocardiographic features in Andersen-Tawil syndrome patients with *KCNJ2* mutations: characteristic T-U-wave patterns predict the *KCNJ2* genotype. *Circulation.* 2005;111:2720–2726.
15. Yan GX, Antzelevitch C. Cellular basis for the normal T wave and the electrocardiographic manifestations of the long-QT syndrome. *Circulation.* 1998;98:1928–1936.
16. Keating M, Atkinson D, Dunn C, Timothy K, Vincent GM, Leppert M. Linkage of a cardiac arrhythmia, the long QT syndrome, and the Harvey Ras-1 gene. *Science.* 1991;252:704–706.
17. Lepeschkin E. The U wave of the electrocardiogram. *Mod Concepts Cardiovasc Dis.* 1969;38:39–45.
18. Jongbloed R, Marcelis C, Velter C, Doevendans P, Geraedts J, Smeets H. dHPLC analysis of potassium ion channel genes in congenital long QT syndrome. *Hum Mutat.* 2002;20:382–391.
19. George CH, Jundi H, Thomas NL, Fry DL, Lai FA. Ryanodine receptors and ventricular arrhythmias: emerging trends in mutations, mechanisms and therapies. *J Mol Cell Cardiol.* 2007;42:34–50.
20. Medeiros-Domingo A, Bhuiyan ZA, Tester DJ, Hofman N, Bikker H, van Tintelen JP, et al. The *RyR2*-encoded ryanodine receptor/calcium release channel in patients diagnosed previously with either catecholaminergic polymorphic ventricular tachycardia or genotype negative, exercise-induced long QT syndrome: a comprehensive open reading frame mutational analysis. *J Am Coll Cardiol.* 2009;54:2065–2074.
21. Itoh H, Shimizu W, Hayashi K, Yamagata K, Sakaguchi T, Ohno S, et al. Long QT syndrome with compound mutations is associated with a more severe phenotype: a Japanese multicenter study. *Heart Rhythm.* 2010;7:1411–1418.
22. Ohno S, Zankov DP, Yoshida H, Tsuji K, Makiyama T, Itoh H, et al. N- and C-terminal *KCNE1* mutations cause distinct phenotypes of long QT syndrome. *Heart Rhythm.* 2007;4:332–340.
23. Hosaka Y, Hanawa H, Washizuka T, Chinushi M, Yamashita F, Yoshida T, et al. Function, subcellular localization and assembly of a novel mutation of *KCNJ2* in Andersen's syndrome. *J Mol Cell Cardiol.* 2003;35:409–415.
24. Zankov DP, Yoshida H, Tsuji K, Toyoda F, Ding WG, Matsuura H, et al. Adrenergic regulation of the rapid component of delayed rectifier K+

current: implications for arrhythmogenesis in LQT2 patients. *Heart Rhythm*. 2009;6:1038–1046.
25. Yoshida H, Horie M, Otani H, Takano M, Tsuji K, Kubota T, et al. Characterization of a novel missense mutation in the pore of *HERG* in a patient with long QT syndrome. *J Cardiovasc Electrophysiol*. 1999;10: 1262–1270.
26. Donaldson MR, Jensen JL, Tristani-Firouzi M, Tawil R, Bendahhou S, Suarez WA, et al. PIP_2 binding residues of Kir2.1 are common targets of mutations causing Andersen syndrome. *Neurology*. 2003;60:1811–1816.
27. Eckhardt LL, Farley AL, Rodriguez E, Ruwaldt K, Hammill D, Tester DJ, et al. KCNJ2 mutations in arrhythmia patients referred for LQT testing: a mutation T305A with novel effect on rectification properties. *Heart Rhythm*. 2007;4:323–329.
28. Fodstad H, Swan H, Auberson M, Gautschi I, Loffing J, Schild L, et al. Loss-of-function mutations of the K(+) channel gene *KCNJ2* constitute a rare cause of long QT syndrome. *J Mol Cell Cardiol*. 2004;37:593–602.
29. Liu XK, Katchman A, Drici MD, Ebert SN, Ducic I, Morad M, et al. Gender difference in the cycle length-dependent QT and potassium currents in rabbits. *J Pharmacol Exp Ther*. 1998;285:672–679.
30. Andelfinger G, Tapper AR, Welch RC, Vanoye CG, George AL Jr, Benson DW. KCNJ2 mutation results in Andersen syndrome with sex-specific cardiac and skeletal muscle phenotypes. *Am J Hum Genet*. 2002;71:663–668.
31. Lopes CM, Zhang H, Rohacs T, Jin T, Yang J, Logothetis DE. Alterations in conserved Kir channel-PIP_2 interactions underlie channelopathies. *Neuron*. 2002;34:933–944.
32. Nehring RB, Wischmeyer E, Doring F, Veh RW, Sheng M, Karschin A. Neuronal inwardly rectifying K(+) channels differentially couple to PDZ proteins of the PSD-95/SAP90 family. *J Neurosci*. 2000;20:156–162.
33. Ma D, Zerangue N, Raab-Graham K, Fried SR, Jan YN, Jan LY. Diverse trafficking patterns due to multiple traffic motifs in g protein-activated inwardly rectifying potassium channels from brain and heart. *Neuron*. 2002;33:715–729.
34. Pfeufer A, Jalilzadeh S, Perz S, Mueller JC, Hinterseer M, Illig T, et al. Common variants in myocardial ion channel genes modify the qt interval in the general population: results from the KORA study. *Circ Res*. 2005;96:693–701.
35. Vega AL, Tester DJ, Ackerman MJ, Makielski JC. Protein kinase A-dependent biophysical phenotype for V227F-*KCNJ2* mutation in catecholaminergic polymorphic ventricular tachycardia. *Circ Arrhythm Electrophysiol*. 2009;2:540–547.
36. Barajas-Martinez H, Hu D, Ontiveros G, Caceres G, Desai M, Burashnikov E, et al. Biophysical and molecular characterization of a novel de novo *KCNJ2* mutation associated with Andersen-Tawil syndrome and catecholaminergic polymorphic ventricular tachycardia mimicry. *Circ Cardiovasc Genet*. 2011;4:51–57.

CLINICAL PERSPECTIVE

Mutations of *KCNJ2*, the gene encoding the human inward rectifier potassium channel Kir2.1, cause Andersen-Tawil syndrome (ATS), a disease exhibiting ventricular arrhythmia, periodic paralysis and dysmorphic features. However, some *KCNJ2* mutation carriers lack the ATS triad and sometimes share the phenotype of catecholaminergic polymorphic ventricular tachycardia (CPVT). We focused on the *KCNJ2* mutation carriers with "atypical ATS phenotype"—patients showing only 1 of ATS features and CPVT phenotype. We investigated the prevalence, clinical, and biophysical characteristics of "atypical ATS" phenotype in *KCNJ2* mutation carriers. *KCNJ2* screening were performed in 57 unrelated probands showing typical (≥2 ATS features) and atypical ATS. We identified 24 *KCNJ2* mutation carriers. Mutation-positive rates were 75% (15/20) in typical ATS, 71% (5/7) in ATS cardiac phenotype alone, 100% (2/2) in periodic paralysis alone, and 7% (2/28) in CPVT. Including 24 *KCNJ2* mutation-positive family members, we divided all carriers (n=45) into 2 groups: typical ATS (A) (n=21, 47%) and atypical phenotype (B) (n=24, 53%). Patients in (A) had a longer QUc interval and higher U-wave amplitude. C-terminal mutations were more frequent in (A). There were no significant differences in incidences of ventricular tachycardia. In patch-clamp analysis using heterologous expression system, the outward IK1 currents of 4 mutations found in (B) showed dominant negative suppression effect although their mild ATS phenotype. *KCNJ2* gene screening in atypical ATS phenotypes is of clinical importance, because more than half (53%) of mutation carriers express atypical phenotypes, despite their arrhythmia severity.

Available online at www.sciencedirect.com

SciVerse ScienceDirect

Journal of Electrocardiology 45 (2012) 770–773

JOURNAL OF Electrocardiology

www.jecgonline.com

Drug-induced QT-interval prolongation and recurrent torsade de pointes in a child with heterotaxy syndrome and *KCNE1* D85N polymorphism☆,☆☆

Lisheng Lin, MD,[a,*] Hitoshi Horigome, MD, PhD,[a] Naoko Nishigami, MD,[a] Seiko Ohno, MD, PhD,[b] Minoru Horie, MD, PhD,[b] Ryo Sumazaki, MD, PhD[a]

[a] *Department of Child Health, Graduate School of Comprehensive Human Sciences, University of Tsukuba, Ibaraki, Japan*

[b] *Department of Cardiovascular and Respiratory Medicine, Shiga University of Medical Science, Shiga, Japan*

Received 18 June 2012

Abstract We present a child case of heterotaxy syndrome (asplenia syndrome) after Fontan procedure that showed extreme prolongation of QT interval and torsade de pointes (TdP) after administration of sodium channel blockers for paroxysmal atrial tachycardia. Despite low serum concentration of the drugs, QT prolongation persisted and TdP attacks with unconsciousness recurred, possibly in association with junctional bradycardia and myocardial damage although he had never experienced QT prolongation during bradycardia before. Temporal cardiac pacing via a venous route to exclude possible implication of bradycardia in induction of TdP was difficult to apply due to total cavopulmonary connection (TCPC) circulation. Continuous intravenous administration of low-dose isoproterenol was started but an appropriate heart rate for prevention of TdP was difficult to obtain. Finally, we were urged to conduct implantation of a DDD pacemaker combined with ICD surgically with epicardial leads, resulting in successful suppression of TdP and syncope. Screening of the genotype disclosed the *KCNE1* D85N polymorphism, which is known as one of the typical disease-causing gene variants in long-QT syndrome (LQTS).

Keywords: Drug-induced long-QT syndrome; Torsade de pointes; *KCNE1* D85N; Sodium channel blocker

Introduction

Antiarrhythmic agents are known to potentially cause QT-interval prolongation and torsade de pointes (TdP), i.e., drug-induced long-QT syndrome (di-LQTS). Recent advancements in molecular biology have revealed that genetic background is often implicated in this life-threatening proarrhythmia.[1] Here, we present a child case of heterotaxy syndrome (asplenia syndrome) after Fontan procedure that showed extreme prolongation of QT interval and recurrent TdP after administration of sodium channel blockers for paroxysmal atrial tachycardia. Screening of the genotype disclosed the *KCNE1* D85N polymorphism, which is known as one of the typical disease-causing gene variants in LQTS.[2]

Case report

A 15-year-old boy was admitted to our hospital because of palpitations. The patient had been diagnosed with heterotaxy syndrome, single atrium, double-inlet single ventricle, pulmonary arterial stenosis, and total anomalous pulmonary venous return (TAPVR), and had undergone total cavopulmonary connection (TCPC) with an extra cardiac conduit combined with TAPVR repair. Electrocardiogram (ECG) on admission revealed atrial tachycardia (AT) with 1:1 atrioventricular conduction (heart rate 150 bpm) although the patient had not previously shown significant arrhythmias, except for transient asymptomatic junctional or sinus bradycardia probably associated with heterotaxy with a heart rate of around 50–60 bpm (Fig. 1). He was hemodynamically stable and medical therapies were started. Repeated intravenous injections of ATP (maximum dose, 0.25 mg/kg) and procainamide (5 mg/kg) failed to convert AT into sinus rhythm. Then, intravenous disopyramide (1 mg/kg) was administered. Eight minutes after the infusion, pulseless tachycardia was suddenly provoked, and a DC shock was applied, resulting in successful conversion. However, AT recurred shortly and therefore continuous infusion of low doses of landiolol (3 μg/kg/min)

☆ This study was conducted at the University of Tsukuba.

☆☆ Grants or financial support for this work: None.

* Corresponding author. Department of Child Health, Graduate School of Comprehensive Human Sciences, University of Tsukuba, 1-1-1 Tenodai, Tsukuba 305-8575, Japan.

E-mail address: lishenglin5433@gmail.com

0022-0736/$ – see front matter © 2012 Elsevier Inc. All rights reserved.
http://dx.doi.org/10.1016/j.jelectrocard.2012.07.013

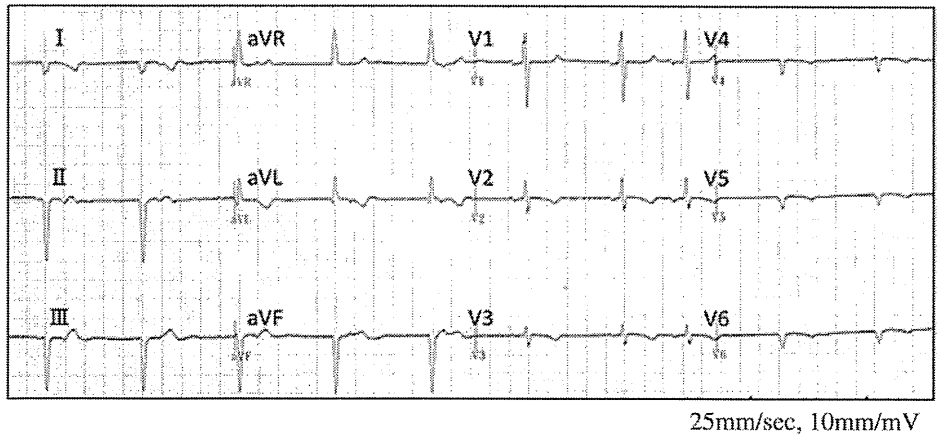

Fig. 1. Baseline 12-lead ECG recorded 3 months before admission, showing junctional bradycardia with a normal QT interval (heart rate 60 bpm, QTc 400 ms).

and digoxin (0.005 mg/kg, twice a day) were started, in order to control the heart rate and to prevent circulatory collapse by recurrence of AT/tachycardia. AT was then under controlled but bradycardia developed gradually and remarkable QT-interval prolongation (QTc ≥ 580 ms) with frequent premature ventricular contraction appeared on ECG monitoring (Fig. 2A and B). Serum levels of potassium, calcium and magnesium were all normal. Although all antiarrhythmic drugs were discontinued, extreme QT prolongation persisted and TdP attacks with unconsciousness recurred (Fig. 2C), necessitating DC shocks several times.

Because immediate application of temporal cardiac pacing via a venous route to exclude possible implication of bradycardia in induction of TdP was difficult to apply due to TCPC circulation, we tried continuous intravenous administration of low doses of isoproterenol. However, an appropriate heart rate for the prevention of TdP was difficult to obtain and a storm of TdP attacks reoccurred. Serum concentration of both procainamide and disopyramide later turned out to be low (0.7 and 0.3 μg/ml at 12 h and 0.5 and, <0.1 μg/ml at 36 h after administration, respectively) compared with their therapeutic ranges (4–10 and 2.8–3.2 μg/ml, respectively). Ultimately, 60 h after admission, we were urged to conduct implantation of a DDD pacemaker combined with ICD surgically with epicardial leads, resulting in successful suppression of TdP and syncope.

A genetic test for LQTS candidate genes revealed the *KCNE1* D85N polymorphism in the index case and in his father (Fig. 3). His mother was negative for the single nucleotide polymorphism (SNP).

Discussion

The present case demonstrated that, even with low serum concentration of sodium channel blocker, marked QT prolongation and recurrent TdP can occur if the patient has other coexistent predisposing factors such as polymorphisms in the LQTS-related genes, as well as bradycardia. Ackerman et al.[3] reported that the allele frequency of the *KCNE1* D85N polymorphism, which was detected in the present case, is approximately 0.7% in healthy Asian populations. According to the survey conducted by Nishio et al.[2] in Japan, its frequency among LQTS probands (3.9%) is significantly higher than that in healthy control subjects (0.81%). This gene polymorphism has recently gathered much interest as a typical culprit of unexpected sudden cardiac death or aborted cardiac death as well as di-LQTS.[4] In an experiment using Xenopus oocytes, I_{Ks} currents were reduced by approximately 50% under heterologous expression of the D85N gene variant.[5] Another functional analysis study using hamster ovarian cells showed that I_{Ks} and I_{Kr} currents of those with the D85N gene variant were reduced by 28% and 31%–36%, respectively.[2]

Sodium channel blocker is one of the most common antiarrhythmic agents used for treatment of tachyarrhythmias. On the other hand, it is also known as one of the typical drugs that provoke di-LQTS/TdP.[1] Sodium channel blocker prolongs both myocardial depolarization and repolarization especially in ischemic or injured regions, enhancing electrical dispersion of myocardium. In the present case, it is difficult to conclude that the significant QT-interval prolongation was caused by *KCNE1* D85N alone. Implication of heterotaxy-related junctional or sinus bradycardia at baseline or some kind of myocardial damage such as clinically unapparent myocarditis in the development of LQT/TdP could not be fully excluded. However, it is unlikely that the latter mechanism alone induced LQT/TdP because the patient had never shown prolonged QT or symptomatic arrhythmias previously even during the phase of marked bradycardia or hemodynamic instability around surgical procedure. It is considered reasonable that *KCNE1* D85N played a significant role as genetic background for development of the life-threatening event in this patient. However, this genetic variance does not seem to have any pathophysiologic relevance to heterotaxy syndrome because we are not aware of any case reports that indicate such association in the literature.

It should be noted that a transvenous approach for temporal pacing is not easy in patients with complex heart disease who have already undergone TCPC in spite of the fact that heterotaxia hearts are often complicated by supraventricular tachycardia, necessitating the use of anti-tachycardia drugs.[6] If a patient with heterotaxy shows episodes of sustained tachycardia, electrophysiological study and catheter ablation of the foci of tachycardia, if necessary, should be conducted before Fontan procedure.

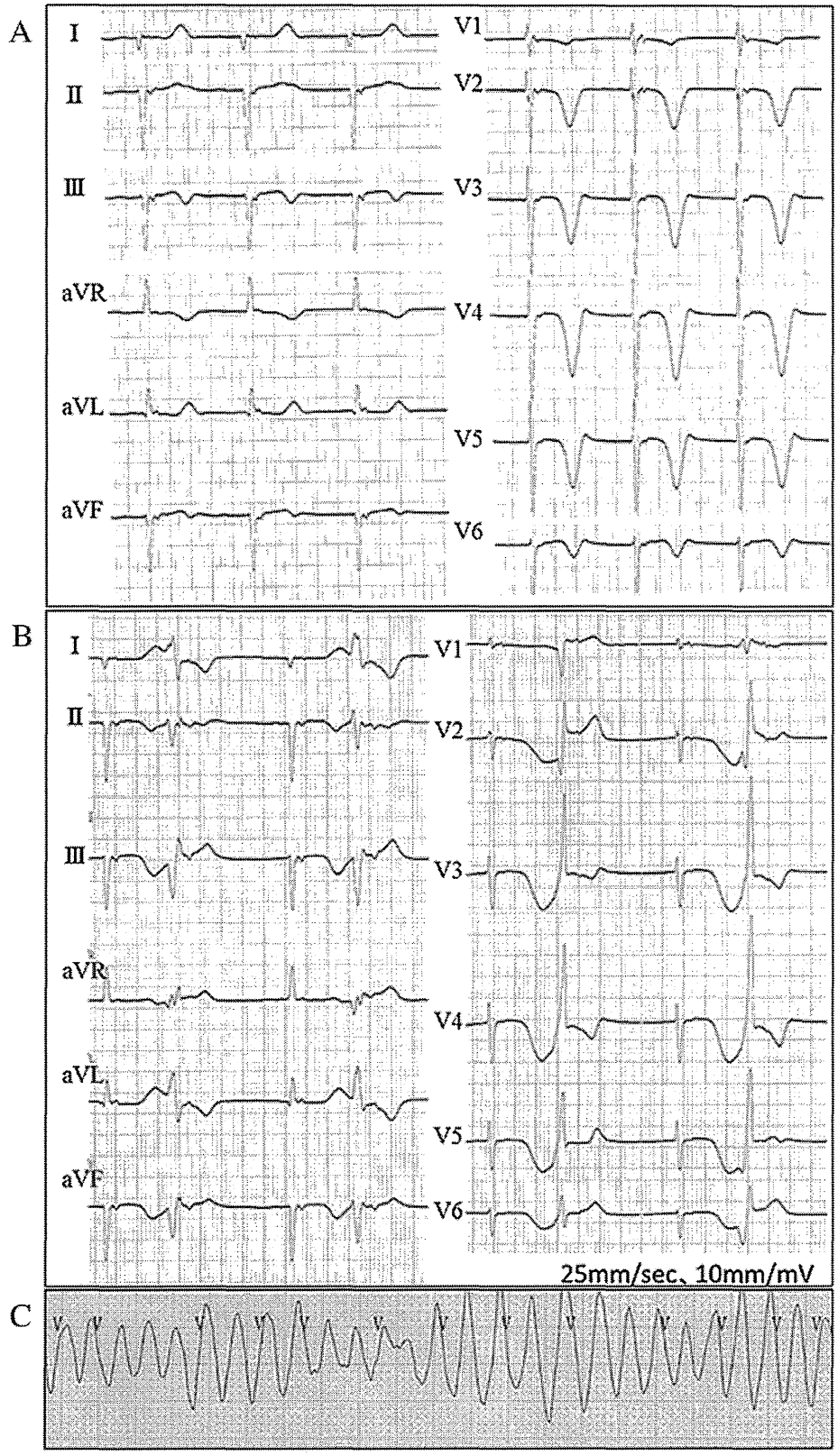

Fig. 2. A: ECG recorded 11h after administration of sodium channel blockers, showing marked QT-interval prolongation with bradycardia (heart rate 60bpm, QTc 580ms). B: ECG showing marked QT-interval prolongation and bigeminy of premature ventricular contraction. C: TdP following extreme QT prolongation.

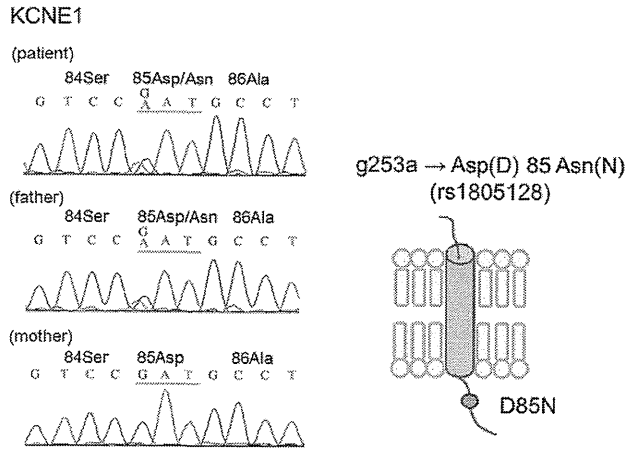

Fig. 3. Representation of direct sequencing of the *KCNE1* of the patient and parents. A G to A transition at codon 253 and resultant amino acid substitution of asparagine for aspartic acid were detected in the index patient and father.

References

1. Itoh H, Sakaguchi T, Ding WG, et al. Latent genetic backgrounds and molecular pathogenesis in drug-induced long-QT syndrome. Circ Arrhythm Electrophysiol 2009;2:511.
2. Nishio Y, Makiyama T, Itoh H, et al. D85N, a KCNE1 polymorphism, is a disease-causing gene variant in long QT syndrome. J Am Coll Cardiol 2009;54:812.
3. Ackerman MJ, Tester DJ, Jones GS, Will ML, Burrow CR, Curran ME. Ethnic differences in cardiac potassium channel variants: implications for genetic susceptibility to sudden cardiac death and genetic testing for congenital long QT syndrome. Mayo Clin Proc 2003;78:1479.
4. Paulussen AD, Gilissen RA, Armstrong M, et al. Genetic variationsof KCNQ1, KCNH2, SCN5A, KCNE1, and KCNE2 in drug-induced long QT syndrome patients. J Mol Med 2004;82:182.
5. Westenskow P, Splawski I, Timothy KW, Keating MT, Sanguinetti MC. Compound mutations:a common cause of severe long-QT syndrome. Circulation 2004;109:1834.
6. Miyazaki A, Sakaguchi H, Ohuchi H, et al. The clinical course and incidence of supraventricular tachyarrhythmias after extra-cardiac conduit Fontan procedures in relation to atrial situs. Circ J 2011; 75:413.

A Connexin40 Mutation Associated With a Malignant Variant of Progressive Familial Heart Block Type I

Naomasa Makita, MD, PhD; Akiko Seki, MD, PhD; Naokata Sumitomo, MD, PhD; Halina Chkourko, MS; Shigetomo Fukuhara, PhD; Hiroshi Watanabe, MD, PhD; Wataru Shimizu, MD, PhD; Connie R. Bezzina, PhD; Can Hasdemir, MD; Hideo Mugishima, MD; Takeru Makiyama, MD, PhD; Alban Baruteau, MD; Estelle Baron, BS; Minoru Horie, MD, PhD; Nobuhisa Hagiwara, MD, PhD; Arthur A.M. Wilde, MD; Vincent Probst, MD, PhD; Hervé Le Marec, MD; Dan M. Roden, MD; Naoki Mochizuki, MD, PhD; Jean-Jacques Schott, PhD; Mario Delmar, MD, PhD

Background—Progressive familial heart block type I (PFHBI) is a hereditary arrhythmia characterized by progressive conduction disturbances in the His-Purkinje system. PFHBI has been linked to genes such as *SCN5A* that influence cardiac excitability but not to genes that influence cell-to-cell communication. Our goal was to explore whether nucleotide substitutions in genes coding for connexin proteins would associate with clinical cases of PFHBI and if so, to establish a genotype-cell phenotype correlation for that mutation.

Methods and Results—We screened 156 probands with PFHBI. In addition to 12 sodium channel mutations, we found a germ line *GJA5* (connexin40 [Cx40]) mutation (Q58L) in 1 family. Heterologous expression of Cx40-Q58L in connexin-deficient neuroblastoma cells resulted in marked reduction of junctional conductance (Cx40-wild type [WT], 22.2±1.7 nS, n=14; Cx40-Q58L, 0.56±0.34 nS, n=14; $P<0.001$) and diffuse localization of immunoreactive proteins in the vicinity of the plasma membrane without formation of gap junctions. Heteromeric cotransfection of Cx40-WT and Cx40-Q58L resulted in homogenous distribution of proteins in the plasma membrane rather than in membrane plaques in ≈50% of cells; well-defined gap junctions were observed in other cells. Junctional conductance values correlated with the distribution of gap junction plaques.

Conclusions—Mutation Cx40-Q58L impairs gap junction formation at cell-cell interfaces. This is the first demonstration of a germ line mutation in a connexin gene that associates with inherited ventricular arrhythmias and emphasizes the importance of Cx40 in normal propagation in the specialized conduction system. **(*Circ Arrhythm Electrophysiol.* 2012; 5:163-172.)**

Key Words: heart block ■ genes ■ ion channels ■ death sudden ■ gap junctions

Cardiac myocyte excitability in atria, His-Purkinje system, and ventricles is largely determined by the properties of voltage-gated sodium channels. Once activated, excitatory currents rapidly propagate to neighboring cells through low-resistance intercellular channels called gap junctions, which facilitate the synchronous contraction of the heart.[1,2] Loss of expression and function of cardiac gap junctions and sodium currents can severely impair action potential propagation, which sets the stage for life-threatening arrhythmias.[1,2] Although multiple mutations in genes coding for components of the voltage-gated sodium channel complex have been previously described in relation to arrhythmias and sudden death in young persons[3] and connexin40 (Cx40) mutations have been implicated in atrial fibrillation,[4,5] no study has identified an

Clinical Perspective on p 172

Received September 24, 2011; accepted January 9, 2012.

From the Department of Molecular Pathophysiology, Graduate School of Biomedical Sciences, Nagasaki University, Nagasaki, Japan (N. Makita); Cardiology, Tokyo Women's Medical University, Tokyo, Japan (A.S., N.H.); Pediatrics and Child Health, Nihon University School of Medicine, Tokyo, Japan (N.S., H.M.); Cardiology, New York University Medical School, New York, NY (H.C., M.D.); Cell Biology, National Cerebral and Cardiovascular Center Research Institute, Suita, Japan (S.F., N. Mochizuki); Cardiology, Niigata University Graduate School of Medical and Dental Sciences, Niigata, Japan (H.W.); Cardiology, National Cerebral and Cardiovascular Center, Suita, Japan (W.S.); Experimental Cardiology, Academic Medical Center, University of Amsterdam, Amsterdam, The Netherlands (C.R.B., A.A.M.W.); Cardiology, Ege University School of Medicine, Bornova, Izmir, Turkey (C.H.); Cardiovascular Medicine, Kyoto University Graduate School of Medicine, Kyoto, Japan (T.M.); l'institut du thorax, INSERM UMR915, Nantes, France (E.B., V.P., H.L., J.-J.S.); Cardiovascular Medicine, Shiga University of Medical Science, Otsu, Japan (M.H.); and Pharmacology and Medicine, Vanderbilt University, Nashville, TN (D.M.R.).

The online-only Data Supplement is available with this article at http://circep.ahajournals.org/lookup/suppl/doi:10.1161/CIRCEP.111.967604/-/DC1.

Correspondence to Naomasa Makita, MD, PhD, Department of Molecular Pathophysiology, Graduate School of Biomedical Sciences, Nagasaki University, 1-12-4 Sakamoto, 852-8523 Nagasaki, Japan. E-mail makitan@nagasaki-u.ac.jp

association between germ line mutations in gap junction proteins and inherited ventricular arrhythmias in humans.

In this study, we investigated a group of patients with progressive familial heart block type I (PFHBI) (Online Mendelian Inheritance in Man 113900), also known as progressive cardiac conduction defect or Lenègre-Lev disease,[6,7] is a dominant inherited disorder of the His-Purkinje system. Affected individuals show electrocardiographic evidence of bundle branch disease (ie, right bundle branch block, left anterior or posterior hemiblock, complete heart block) with broad QRS complexes. The disease can progress from a normal ECG to right bundle branch block and from the latter to complete heart block. Affected individuals often present with family history of syncope, pacemaker implantation, and sudden death.[8] Although structural abnormalities have been invoked as a cause of the disease,[6,7] a number of patients present with normal cardiac structure and contractile function. Linkage analysis in a large South African PFHBI kindred[9] and a Lebanese kindred[10] mapped a causal locus on chromosome 19q13.3, and further work identified mutations in genes encoding for the transient receptor potential nonselective cation channel, subfamily M, member 4 (*TRPM4*) gene[11] at this locus. Haploinsufficiency of *SCN5A* and aging have been implicated in PFHBI,[8] and age-dependent manifestations of the disease have been recapitulated in mice.[12]

Here, we sought to expand on the association between PFHBI and mutations in genes relevant to action potential propagation; in particular, we assessed the possible association between nucleotide substitutions in connexin-coding genes and PFHBI. We evaluated 156 probands of diverse ethnic backgrounds from Asia, Europe, and North America given a clinical diagnosis of PFHBI. In addition to the sodium channel mutations previously reported,[13–15] we identified a germ line missense mutation in *GJA5* in a family with severe, early onset disease. This gene codes for the gap junction protein connexin40 (Cx40), which predominantly expresses in the atria and His-Purkinje system.[16] Heterologous expression experiments revealed that this novel mutation (Cx40-Q58L) significantly impaired the ability of Cx40 to form gap junction channels. Confocal microscopy showed that the Cx40-Q58L mutant but not the wild type (WT) failed to form plaques at sites of cell-cell apposition. Coexpression experiments indicated that the Cx40-WT protein provided only partial rescue of the Cx40-Q58L cellular phenotype. To our knowledge, this is the first description of a germ line mutation in a connexin gene associated with inherited ventricular arrhythmias. The results open the possibility of *GJA5* as a candidate gene for screening in patients with PFHB1, yet in the absence of further evidence, screening may be limited to the research environment rather than included as a part of the routine diagnostic examination.[17] The data also emphasize the importance of Cx40 in the maintenance of normal propagation in the specialized conduction system of the human heart.

Methods

Genetic Screening of PFHB1

Genomic screening by polymerase chain reaction and DNA sequencing was performed for *GJA5* (Cx40), *GJA1* (Cx43), *GJC1* (Cx45), *KCNQ1, KCNH2, SCN5A, KCNE1, KCNE2, KCNJ2, SCN1B, SCN4B, HCN4*. Primer information is provided in the online-only Data Supplement. All participating probands and family members gave written informed consent in accordance with standards (Declaration of Helsinki) and local ethics committees.

Plasmid Construction

A 1.1-kb Cx40-DNA fragment was subcloned into bicystronic plasmids pIRES2-EGFP and pIRES2-DsRED2. An EGFP or FLAG epitope was added at Cx40 C terminal to generate EGFP- or FLAG-tagged Cx40. Site-directed mutagenesis (Q58L) was performed with QuikChange. Primer information and additional details are provided in the online-only Data Supplement.

Cell Culture and Transfection

Constructs were introduced into connexin-deficient HeLa cells or mouse neuroblastoma (N2A) cells using Lipofectamine as per manufacturer's protocol.

Electrophysiology

Gap junction currents were recorded from transiently transfected N2A cell pairs using whole-cell double-patch clamp techniques as previously described.[18,19] Further details are provided in the online-only Data Supplement.

Immunocytochemistry and Western Blotting

HeLa cells, transfected with pEGFPN1-Cx40-WT, pCMV-FLAG-Cx40-Q58L, or both, were stained with anti-FLAG M2 antibody and Alexa546-labeled secondary antibody. EGFP and Alexa546 fluorescence images were recorded by confocal microscopy. For western blotting, N2A cells were transiently transfected with 3 μg of Cx40 plasmids. Two days after transfection, cells were lysed, and proteins were extracted and separated by conventional methods. Further details are provided in the online-only Data Supplement.

Statistical Analysis

Results are presented as mean±SEM. Mann-Whitney rank sum tests with Bonferroni post hoc correction were used in comparisons for which normality or equal variance assumptions were invalid. In other instances, differences between groups were assessed by 1-way ANOVA followed by Bonferroni post hoc correction. Statistical significance was assumed for $P<0.05$.

Results

Genetic Screening of PFHBI Probands

We genetically screened 156 probands given a clinical diagnosis of PFHBI. We identified 4 novel and 5 previously reported mutations in *SCN5A*,[13,15] 3 mutations in *SCN1B*,[14] and a novel germ line heterozygous missense mutation in exon 2 of the Cx40 gene *GJA5* (online-only Data Supplement Table I). Mutations were not found in connexin genes *GJA1* (Cx43) or *GJC1* (Cx45) or in the other genes screened (*KCNQ1, KCNH2, KCNE1, KCNE2, KCNJ2, HCN4,* or *SCN4B*). Of the novel *SCN5A* mutations, 1 caused a modification of the amplitude and voltage gating kinetics of the sodium current in heterologously expressing cells (online-only Data Supplement Figure I); 3 other mutant constructs failed to express functional channels, suggesting that patients carrying the mutation were functionally haploinsufficient for Nav1.5 (online-only Data Supplement Figure I). The *GJA5* mutation (c.173A>T) caused an amino acid substitution (glutamine [Q] replaced by leucine [L]) at position 58 in Cx40 (Cx40-Q58L) (Figure 1A and 1B). The mutation was absent in 400 alleles from unaffected control subjects and in the other 155 PFHBI probands. Screening of the entire gene

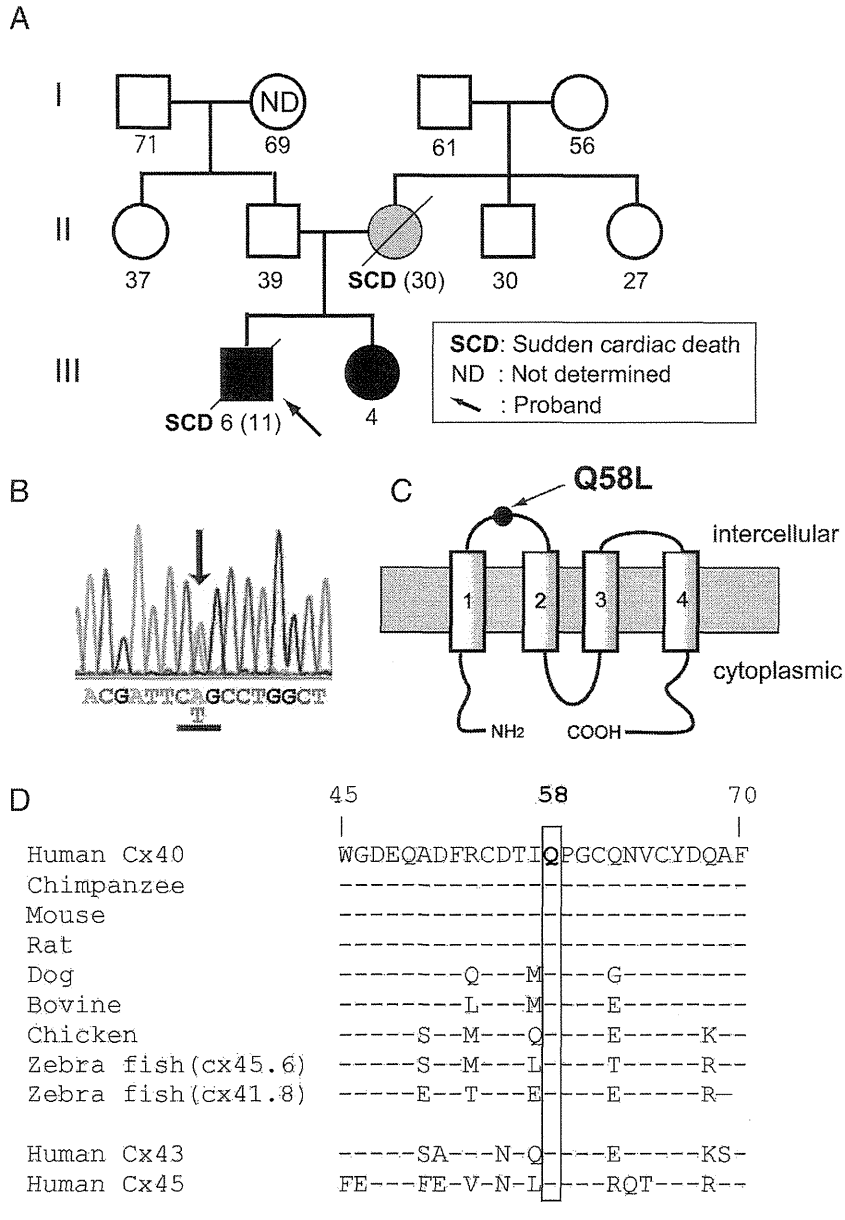

Figure 1. *GJA5* mutation identified in a family given the clinical diagnosis of progressive familial heart block type I. **A**, Family pedigree. Genetically affected and unaffected individuals are shown with closed and open symbols, respectively. The hatched circle indicates the proband's mother not genotyped; clinical data suggest that she was a de novo mutation carrier. Number below each symbol indicates the age at registration or age of SCD (parenthesis). **B**, Sequence electropherogram of exon 2 *GJA5* of proband. Arrow indicates heterozygous missense mutation of leucine (CTG) for glutamine-58 (CAG). **C**, Cx40 predicted membrane topology indicating position Q58 in first extracellular loop. **D**, Sequence alignment of human Cx40 and its homologues (residues 45–70). Notice the conservation in human Cx43 and Cx45. Dashes indicate residues identical with the top sequence. Cx indicates connexin.

panel (including *SCN5A* and *SCN1B*) revealed no other sequence modification in the DNA of this proband. Topological analysis placed amino acid 58 of Cx40 within the first extracellular loop (Figure 1C). The presence of glutamine in this position is highly conserved among *GJA5* orthologs, and 2 other cardiac connexins, Cx43 and Cx45 (Figure 1D). The clinical and genotypic characteristics of proband and tested family members are described next.

Clinical Phenotypes and Genotype of the PFHBI Pedigree With the *GJA5* Mutation

The proband, an 11-year-old boy at time of death, was first referred for evaluation when he was age 6 years because of ECG abnormalities. Although asymptomatic at that time, his ECG showed advanced atrioventricular block, complete left bundle branch block, and left axis deviation (Figure 2A). Echocardiography and cardiac scintigraphy did not reveal signs of structural heart disease. He experienced an episode of syncope at age 9; implantation of a permanent pacemaker was recommended by the physician but not authorized by the legal guardian. The proband died suddenly 2 years later during exercise (running), and the family declined postmortem examination. The proband's younger sister shares the Cx40-Q58L mutation. She is asymptomatic, with a QRS duration at the upper limit of normal, left axis deviation that has been progressive (online-only Data Supplement Table II), and QRS notch. These findings are consistent with impaired intraventricular conduction (Figure 2B). The mother died suddenly at age 30 after delivering the second child. An ECG on record, obtained when she was age 16, was similar to that of the proband (compare Figure 2C with 2A). In addition, a ventricular tachycardia was recorded during the recovery phase of an exercise stress test (online-only Data Supplement Figure II). DNA from the mother was not available for

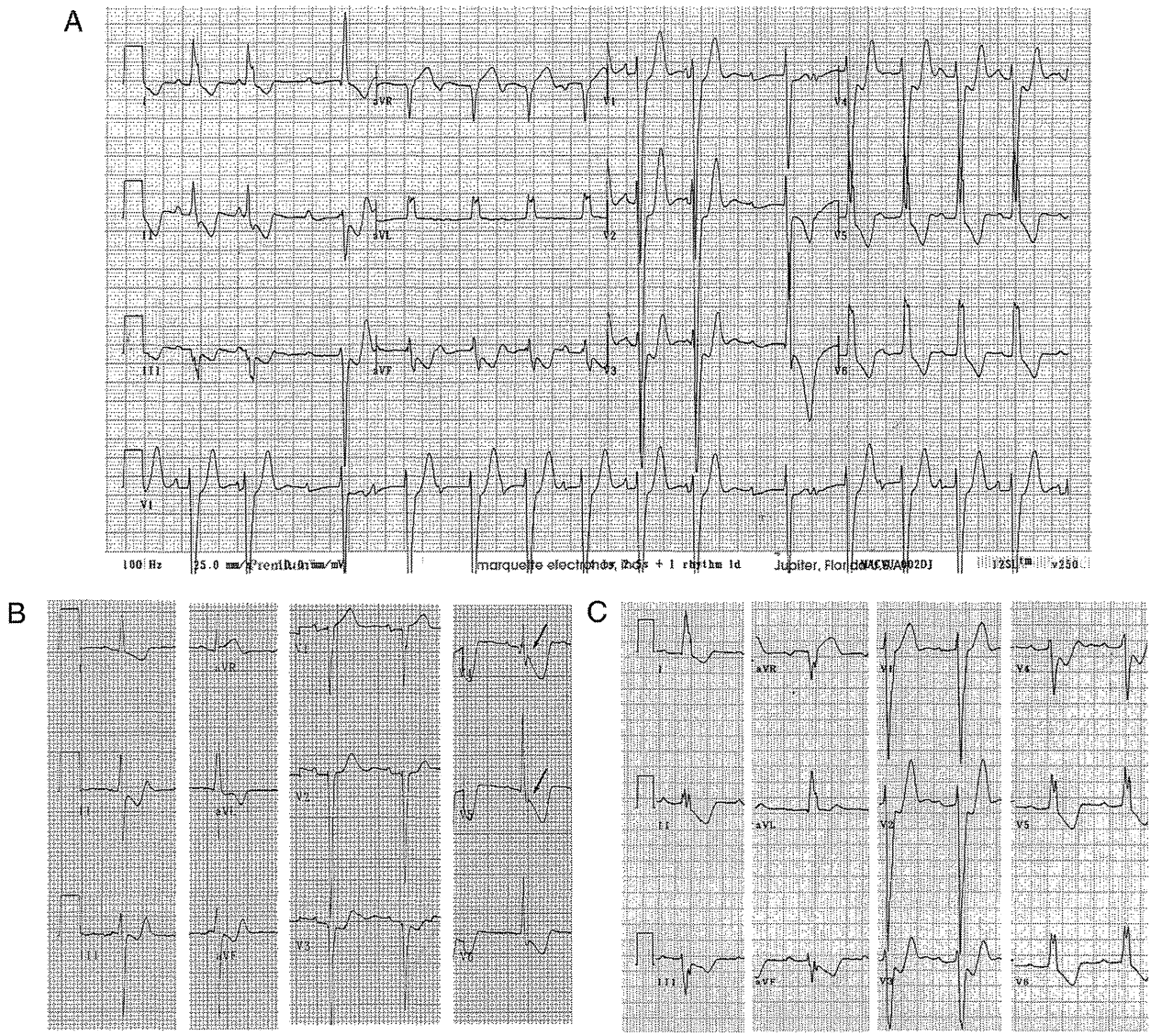

Figure 2. ECGs of proband and affected family members. **A**, ECG of proband at age 6 years, showing advanced atrioventricular block, complete left bundle branch block, and left axis deviation. Patient died suddenly 5 years later. **B**, ECG of proband's sister at age 6 years, showing QRS duration at the upper limit of normal, left axis deviation that has been progressive, and QRS notch in leads V4 and V5 (arrows) consistent with impaired intraventricular conduction. **C**, ECG of proband's mother at age 16 years, showing complete left bundle branch block and left axis deviation. She died suddenly at age 30.

examination. Other family members, including the proband's father, showed normal ECGs. DNA analysis of proband's father and maternal grandparents revealed absence of the Cx40-Q58L mutation. On the basis of clinical data and genotypic features of the proband and sister, it is most likely that the Cx40-Q58L mutation appeared de novo in the proband's mother. The data also indicate an early onset of PFHBI in this family compared with the natural history of the disease in most other cases.[8] As an initial step to assess the functional implications of the Cx40-Q58L mutation, modified constructs were transiently expressed in an exogenous system and evaluated for localization and function.

Electrophysiological Properties of Mutant Cx40-Q58L Channels

Connexin-deficient N2A cells were transiently transfected with cDNA for Cx40-WT or Cx40-Q58L; electrophysiological properties of homologous Cx40 channels were analyzed by conventional dual whole-cell patch clamp. Figure 3A shows representative junctional current traces elicited by a transjunctional voltage gradient of −60 mV. Average junctional conductance (Gj) decreased from 22.2±1.7 nS in cells expressing Cx40-WT (n=14) to 0.56±0.34 nS in cells expressing the Cx40-Q58L mutant (n=14; $P<0.001$). The probability of functional coupling, calculated by dividing the number of electrically coupled pairs by the number of pairs tested, was 100% and 57.1% for Cx40-WT and Cx40-Q58L, respectively.

Figure 3B depicts representative single-channel recordings elicited by a transjunctional voltage of −60 mV in cell pairs expressing Cx40-WT or Cx40-Q58L. Unitary events for WT channels displayed current transitions corresponding to 2 conducting states (O_1 and O_2) of 43.3 and 119.5 pS, respectively. Figure 3C shows the event histograms for both cell

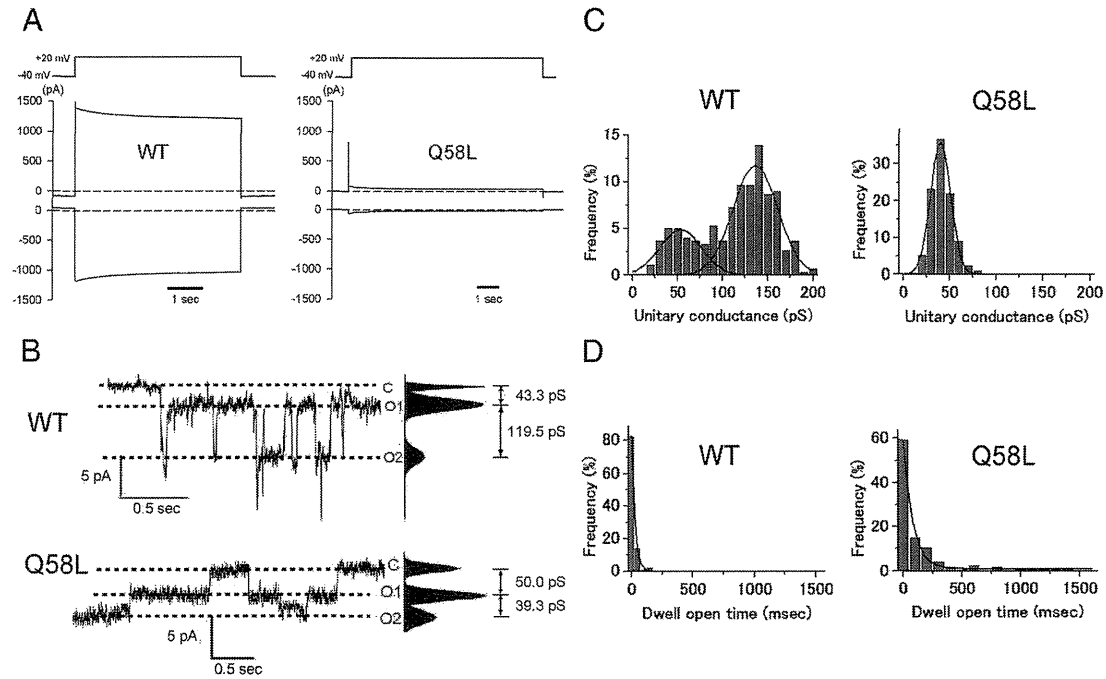

Figure 3. Whole-cell and single-channel properties of connexin40 (Cx40)-WT and Cx40–Q58L channels. **A**, Voltage pulse (top) and junctional current (bottom) from a homomeric WT cell pair (junctional conductance, 12.9 nS) and a Q58L cell pair (junctional conductance, 1.2 nS). **B**, Unitary currents recorded from homomeric Cx40-WT and Cx40–Q58L channels. O_1 and O_2 refer to 2 conducting (open) unitary levels of current. **C**, All-event histograms pooled from WT (n=3) and Q58L (n=3) cells with homologous channels. For WT, Gaussian peaks centered at 136.2±2.3 and 53.1±5.3 pS. For Q58L, best fit by a single Gaussian distribution centered at 40.2±0.3 pS (n=3). **D**, Frequency of events in relation to dwell open time. Binned data were fit by single exponentials (τ_{open} WT, 27.9±0.5 ms, 4 cells, 186 events; τ_{open} Q58L, 92.0±7.8 ms, 3 cells, 163 events). WT indicates wild type.

types (Cx40-WT, 3 cell pairs and 303 events; Cx40-Q58L, 3 cell pairs and 416 events). The histogram for the Cx40-WT channels was best described by 2 Gaussian distributions centered at 136.2±2.3 and 53.1±5.3 pS. In contrast, the histogram for Cx40-Q58L channels was best described by a single Gaussian function centered at 40.2±0.3 pS. Moreover, the length of time that a channel dwelled in the open state (dwell open time) was substantially longer for the Cx40-Q58L channels (92.0±7.8 ms, 3 cell pairs, 163 events) than for Cx40-WT channels (27.9±0.5 ms, 4 cell pairs, and 186 events) (Figure 3D). Of note, the Q58L mutation had a strong dominant effect on formation of heterotypic functional gap junctions. Cells were transfected with either pIRES2-EGFP-Cx40-WT or pIRES2-DsRED2-Cx40-Q58L, and heterotypic pairs were identified by fluorescence microscopy (an EGFP-expressing cell paired with a DsRED2-expressing cell). We recorded from 8 cell pairs and detected unitary current events in only 2 pairs. A total of 57 events were recorded, and average macroscopic junctional conductance was 0.04±0.03 nS. Collectively, the data demonstrated that the Q58L mutation significantly affects the biophysical properties of Cx40 channels and the overall ability of Cx40 gap junctions to form a low-resistance pathway between cells.

Electrophysiological Properties and Gap Junction Plaque Formation in Cells Coexpressing WT and Q58L Proteins

In the clinical cases identified, the Q58L mutation was detected in only 1 carrier allele. Therefore, we assessed the function of gap junctions in cells coexpressing WT and mutant proteins. N2A cells were cotransfected with cDNA for both GFP-tagged Cx40-WT and Cx40-Q58L (0.5 μg of pEGFPN1-Cx40-WT combined with 0.5 μg of pEGFPN1-Cx40-Q58L). Results were compared with those obtained when only 1 of the constructs (1 μg) was transfected. Cells expressing both constructs (WT/Q58L) showed intermediate conductance (15.4±3.7 nS, n=16) between WT (28.8±3.6 nS, n=16, $P<0.001$) and Q58L (0.28±0.11 nS, n=14, $P<0.001$) (Figure 4A). These values were comparable to those obtained using the bicistronic pIRES2-EGFP constructs (WT, 22.2±1.7 nS, n=14; WT/Q58L, 13.0±2.4 nS, n=17; Q58L, 0.56±0.34 nS, n=14). The coexpression results were consistent with those obtained using pIRES plasmids that tagged the cells both green and red, if cotransfected (online-only Data Supplement Figure I). The probability of finding functional coupling in cotransfected cells was 76.5%, which was intermediately between WT (100%) and Q58L (57.1%).

The characteristics of gap junction plaques observed in cells coexpressing WT and Q58L varied significantly between pairs (Figure 4B). Nearly one half of transfected (fluorescence-positive) cells exhibited clear and discrete gap junction plaques (arrow a), whereas the rest of fluorescent-positive cells showed a diffuse expression pattern and absence of well-defined plaques (arrow b). Fluorescence-positive and gap junction plaque-positive cells were counted in 10 different views for each group, and efficacy of gap junction plaque formation was statistically analyzed (Figure 4C) by calculating the ratio of cells with gap junction plaques

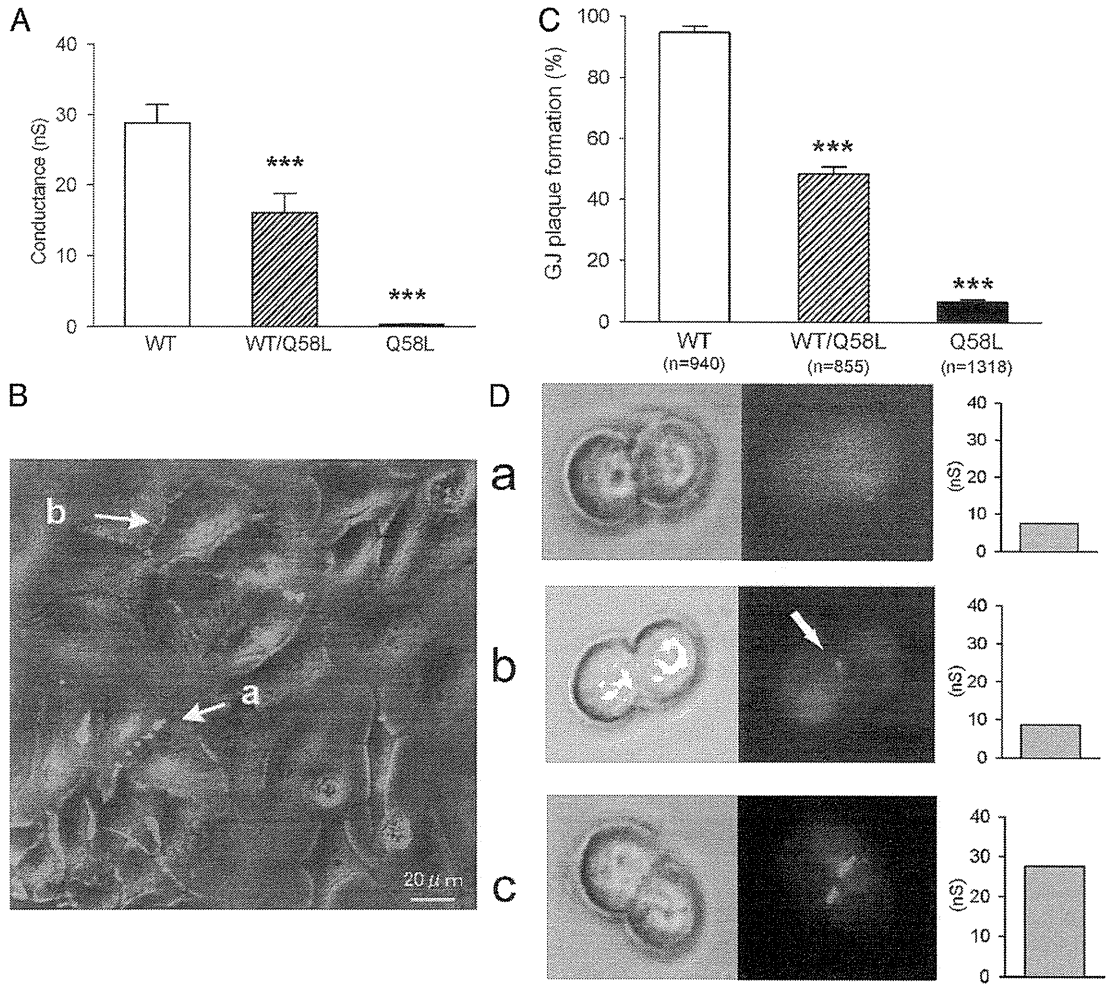

Figure 4. Macroscopic conductance and gap junction plaque morphology in cells coexpressing connexin40 (Cx40)-WT and Cx40-Q58L. **A**, Junctional conductance of cells transfected with plasmid pEGFPN1-Cx40-WT (1 μg), pEGFPN1-Cx40-Q58L (1 μg), or cotransfected with WT and Q58L (WT/Q58L, pEGFPN1-Cx40-WT 0.5μg+pEGFPN1-Cx40-Q58L 0.5 μg). **B**, Phase contrast/fluorescence overlay image of neuroblastoma cells transfected with WT/Q58L constructs. Arrow *a* points to gap junction plaque; arrow *b* points to an example of cells transfected but devoid of gap junction plaque. **C**, Efficacy of gap junction plaque formation was measured as the ratio between the number of gap junction plaque-positive cells and the number of fluorescent-positive cells (WT, n=940; WT/Q58L, n=855; Q58L, n=1318). **D**, Representative images of phase contrast (left), EGFP fluorescence (middle), and junctional conductance (right) from neuroblastoma cells cotransfected with pEGFPN1-Cx40-WT (0.25 μg) and pEGFPN1-Cx40-Q58L (0.25 μg). Three different examples illustrate the relation between plaque morphology and recorded junctional conductance. WT indicates wild type. ***$P<0.001$ compared with WT.

to the number of fluorescence-positive cells. In the Cx40-WT group, almost all fluorescent-positive cells exhibited clear gap junction plaques (94.9±1.9%, n=940), whereas there was a more-diffuse and homogenous pattern with only occasional plaque formation in the Cx40-Q58L group (6.6±0.7%, n=1318, $P<0.001$ compared with WT). In contrast, results varied widely in cells cotransfected with WT/Q58L; nearly one half of fluorescence-positive cells exhibited gap junction plaques similar to those observed in cells transfected with the WT construct (48.2±2.4%, n=855, $P<0.001$), whereas the rest showed a diffuse expression pattern similar to that of Cx40-Q58L. To establish a better correlation between plaque formation and junctional conductance, both variables were measured concurrently in the same cell pair for 39 N2A cell pairs where GFP-tagged plasmids of Cx40-WT and Cx40-Q58L were cotransfected. As shown in Figure 4D, about one half of GFP-positive cell pairs showed a very small Gj (<5 nS) and very few or negligible gap junction plaques (a). In the other half of cell pairs, small, dot-like junctional plaques correlated with intermediate Gj values (b), and there were clear, extensive gap junction plaques associated with Gj values >25 nS (c). Overall, we found significant heterogeneity in the extent of electric coupling, although the measurements of Gj correlated with the localization of proteins in transfected cells. These results indicate that the Q58L mutation significantly impairs the ability of cells to form gap junction plaques, although the effect is not purely dominant when both WT and mutant proteins are coexpressed.

Subcellular Distribution of WT and Q58L Cx40 in Transiently Transfected Cells

To further analyze the subcellular distribution of Cx40-WT and Cx40-Q58L proteins, the C terminal of Cx40-WT was

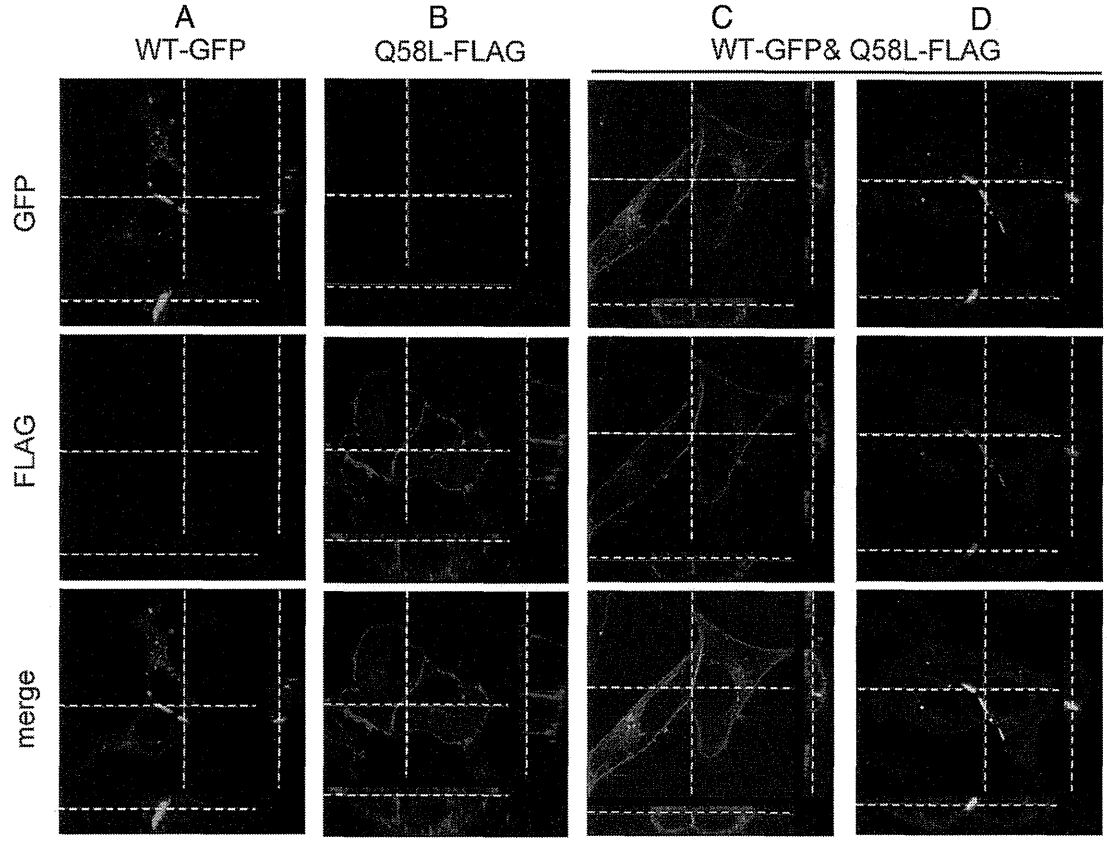

Figure 5. Subcellular distribution of connexin40 (Cx40)-WT and Cx40-Q58L in transiently transfected cells. HeLa cells were transiently transfected with pEGFPN1-Cx40-WT (3.0 μg) (**A**), pCMV-FLAG-Cx40-Q58L (3.0 μg) (**B**), or pEGFPN1-Cx40-WT (1.5 μg) plus pCMV-FLAG-Cx40-Q58L (1.5 μg) (**C**); immunostained for the respective tag protein; and visualized by confocal laser scanning microscopy. Notice that gap junction plaques (**A**) are absent in Q58L transfectants (**B**) and present in some (**D**) but not all (**C**) cotransfected cells. Bar=20 μm. WT indicates wild type.

tagged with GFP, whereas the C terminal of Cx40-Q58L was FLAG tagged. After transfection of N2A cells with the tagged constructs, the distribution of each protein was examined by confocal microscopy. As shown in Figure 5, green color indicates the position of GFP-tagged molecules, whereas red indicates the position of FLAG-tagged molecules. In cells transfected only with GFP-tagged Cx40-WT, fluorescence was consistently detected at sites of cell-cell apposition, following the pattern previously described for GFP-labeled gap junction plaques (Figure 5A). A similar distribution was found when cells were transfected with FLAG-tagged Cx40-WT (not shown). In contrast, most FLAG-tagged Cx40-Q58L signals were evenly distributed around the cell in the vicinity of the plasma membrane (Figure 5B). Biotinylation experiments showed that the Q58L mutation did not prevent the Cx40 protein from inserting into the membrane and presenting a domain-reachable form in the extracellular space (online-only Data Supplement Figure II). Micoscopy experiments in cells coexpressing GFP-tagged Cx40-WT and FLAG-tagged Cx40-Q58L proteins yielded results intermediate to those obtained when only 1 construct was expressed. Nearly one half of cell pairs showed that both proteins distributed homogenously at or near the cell membrane, without the formation of well-defined gap junction plaques (Figure 5C). These images resembled those obtained when only Cx40-Q58L proteins were expressed (Figure 5B, FLAG). In contrast, other cell pairs showed clustering of fluorescent signals within closely confined areas that appeared to be gap junction plaques (Figure 5D).

The experiments described herein led us to speculate that the distribution and function of heteromeric connexons is determined by their mutant subunit content, whereby formation (or not) of plaques and channels are determined, at least in part, by the abundance of expression of one protein over the other. As an initial step to probe this hypothesis, we took advantage of the characteristics of the bicistronic plasmid pIRES, in which the expression rate of the upstream gene is several-fold greater than that of the downstream gene,[20] and explored the functional properties of heteromeric connexons. Cx40-WT and GFP-tagged Cx40-Q58L were subcloned into the pIRES vector, either alone or in combination, in the specific orientations shown in Figure 6A. Protein expression levels of Cx40-WT and Cx40-Q58L were determined by immunochemistry. In contrast to the data obtained when Cx40-WT and GFP-tagged Cx40-Q58L plasmids were cotransfected at a 1:1 ratio (lane 6), expression of heteromeric pIRES plasmids WT-IRES-Q58L-EGFP (lane 3) and Q58L-EGFP-IRES-WT (lane 4) resulted in uneven protein expression levels of WT (40 kDa) and Q58L-EGFP (67 kDa), depending on their orientation in the pIRES vector. Based on

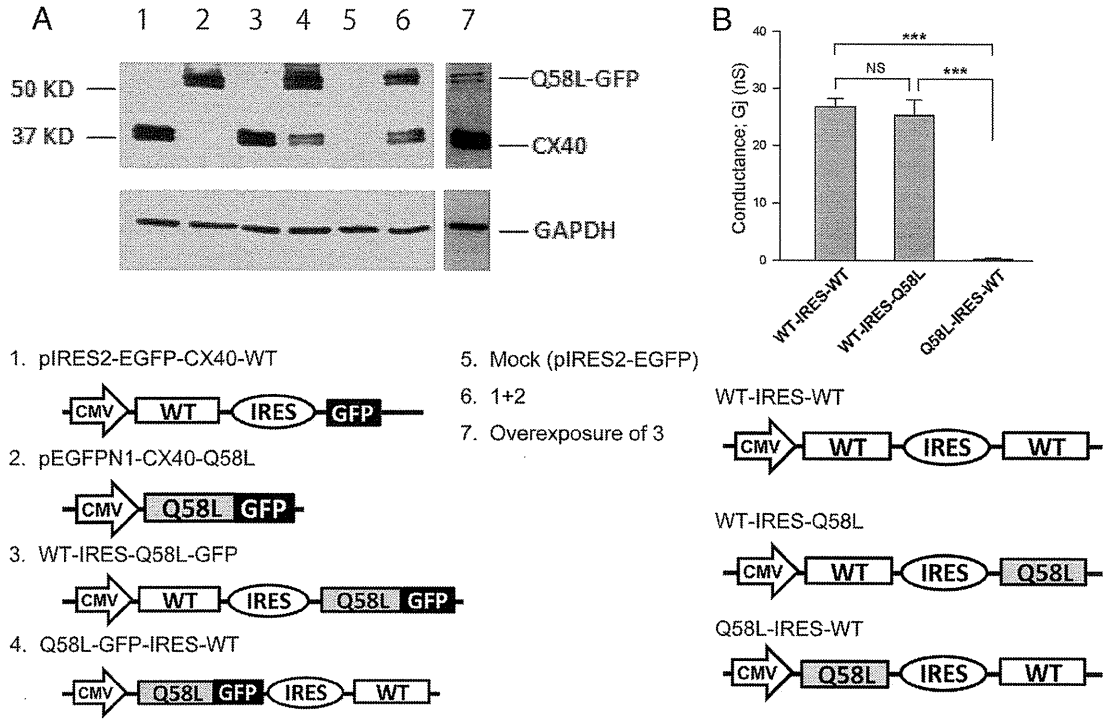

Figure 6. Mutant subunit abundance correlated with gap junction function. **A**, Neuroblastoma cells were transiently transfected with 3 μg Cx40 constructs in IRES plasmids. Cell lysates were analyzed by western blot using anti-Cx40 (top) and anti-GAPDH antibodies (bottom). The number in each lane corresponds to the plasmid noted below the image. Samples from cells cotransfected with plasmids 1 and 2 (1.5 μg each) were loaded on lane 6. Double bands of Cx40-WT (40 kDa) and Q58L-EGFP (67 kDa) are shown in lanes 3, 4, 6, and 7. Results were repeated in 3 separate experiments. Overexposure (lane 7) confirmed expression of the high-molecular-weight protein in lane 3. **B**, Junctional conductance of homomeric and heteromeric constructs (WT-IRES-Q58L and Q58L-IRES-WT). Conductance of cell pairs expressing WT-IRES-WT (n=17) was comparable to heteromeric construct WT-IRES-Q58L (n=17). However, converse heteromeric construct Q58L-IRES-WT (n=15) showed significantly reduced conductance ($P<0.001$ versus WT-IRES-WT and WT-IRES-Q58L). ***$P<0.001$. NS indicates not significant; WT, wild type.

these observations, we constructed a homomeric Cx40-WT plasmid (WT-IRES-WT) and heteromeric plasmids of Cx40-WT and Cx40-Q58L with different orientations (WT-IRES-Q58L and Q58L-IRES-WT) (Figure 6B). The junctional conductance of cell pairs expressing WT-IRES-Q58L (25.3±2.8 nS, n=17) was nearly indistinguishable from that of the homomeric plasmid WT-IRES-WT (27.8±1.4 nS, n=17, *P* not significant). By contrast, the converse heteromeric construct Q58L-IRES-WT showed substantially reduced junctional conductance (0.29±0.12 nS, n=15, $P<0.001$) comparable with that of the homomeric Q58L (0.56±0.34 nS) (Figure 3A). These results suggest that the final electrophysiological properties of the heteromeric connexons are determined predominantly by the numbers of mutant subunits in each gap junction rather than defined by a dominant-negative effect.

Discussion

Genetic screening confirmed the association of *SCN5A* and *SCN1B* with PFHB1[13–15] and revealed novel mutations within these genes (online-only Data Supplement Table I). More importantly, we identified a particularly severe, early onset case of PFHBI associated with a germ line mutation in *GJA5* in 2 blood relatives (proband and sister) given a clinical diagnosis of PFHBI. The data also indicate that the protein expressed (Cx40-Q58L) failed to form functional gap junctions in an exogenous expression system and decreased the probability of gap junction formation in cells coexpressing the WT protein.

So far, *SCN5A*, *SCB1B*, and *TRPM4* are the only genes associated with PFHB1.[11,13,14] The National Human Genome Research Institute database shows no association of *GJA5* single-nucleotide polymorphisms with arrhythmias or conduction system diseases. PR interval and QRS have been associated with several loci, including *SCN5A*, *SCN10A*, *NKX2.5*, and *TBX5*[21,22] but not *GJA5*, which is located at chromosome 1q21.1. Overall, the present results suggest that *GJA5* is a candidate gene associated with PFHBI, likely in a small fraction of the affected population. Yet, given the limited cosegregation observed in the reported family, we remain cautious in assigning a causative nature to the *GJA5* mutation. It will be of great interest to expand the screening of *GJA5* at the research level to identify other cases associated with amino acid changes in Cx40, although it may be premature to include *GJA5* as a part of the routine diagnostic screen.[17] The present results also emphasize the importance of Cx40 in the maintenance of normal cardiac rhythm.

To our knowledge, this is the first report of a germ line mutation in Cx40 associated with a high risk of ventricular arrhythmias (online-only Data Supplement Figure II). Other studies have shown somatic mutations of Cx40 or Cx43 in patients with idiopathic atrial fibrillation[5,23]; those mutations

were confined to the atria, and conduction abnormalities in the ventricles or His-Purkinje system were not observed. On the other hand, as in all cases involving identified genetic substrates for disease, the possibility of compound mutations in unexamined genes cannot be excluded. We do emphasize that the mutation led to a severe cellular phenotype in an exogenous expression system, supporting the argument that just the Q58L substitution can impair the formation of gap junctions necessary for propagation of action potentials between cells.

The results show that Cx40-Q58L was abundantly expressed in an exogenous system. The protein reached the vicinity of the cell membrane but failed to form gap junction plaques (Figure 5B). This result may be due to impaired docking of mutant hemichannels within the intercellular space because of the mutation in the extracellular loop (Figure 1C). During trafficking, connexin subunits oligomerize to form a hemichannel (or connexon). Once at the site of cell contact, connexons from apposing cells dock, sealing the hydrophilic path (the channel pore) from the extracellular space. The locking of 2 connexons into 1 gap junction channel is believed to stabilize connexin subunits in place, facilitating aggregation of other oligomers into their vicinity and eventually forming a plaque. Amino acid substitutions within the extracellular loop, as in Q58L, can prevent hemichannel docking and, thus, plaque formation.[24] The present biotinylation experiments indicate that the Q58L protein integrates into the cell membrane, supporting the notion that the inability of the Q58L mutation to form functional gap junctions is related to events that occur after the oligomer is delivered to the cell membrane and before a functional dodecamer converts into a functional channel in a gap junction plaque.

Results obtained in cells coexpressing both mutant and WT proteins clearly show that one subunit can significantly influence the fate of the other (Figure 5). This suggests that Cx40-Q58L subunits retain their ability to oligomerize not only with other mutant subunits, but also with the WT protein. The results also present an interesting paradigm in that neither the WT nor the mutant construct exerted a dominant effect over the other. After transfection with equal amounts of cDNA, we found cells where both WT and mutant proteins displayed the phenotype of the mutant construct, whereas in other cases, junctional plaques could be easily discerned (although an outline of the cell, likely resulting from the presence of the FLAG-tagged mutant protein, could still be observed [see red signal in Figure 5D]). These results can be explained if we assume that the probability of proper targeting and integration of a connexon into a plaque decreases as a function of the number of mutant subunits contained. For cotransfection, we used equal amounts of cDNA; however, it is very likely that each cell was transfected with variable amounts of each construct and, thus, expressed variable amounts of each protein. We speculate that a majority (though of unknown stoichiometry) of WT connexin subunits are required in a connexon for proper formation of functional gap junctions. Thus, if a cell captures an abundance of Q58L cDNA, most oligomers will contain an excess of mutant subunits, and gap junction formation will fail. If, on the other hand, that cell captures and expresses more of the WT cDNA, the distribution of the subunits within the oligomer will contain a majority of WT connexins, and the connexon will be properly integrated into a channel. This hypothesis will require further testing, although data presented in Figure 6 support the concept that success or failure of functional channel formation may relate to relative abundance of each protein (WT or mutant). If our hypothesis is correct, it suggests that the distribution of functional gap junctions in the His-Purkinje network of affected individuals could vary significantly among cells, depending on the extent of expression of each allele in each cell. The resulting phenotype may be that of a Purkinje network where gap junction-mediated coupling could be heterogeneous, setting the stage for local conduction block, microreentry, and ventricular arrhythmias at the Purkinje network or at the Purkinje-muscle junction.[1,2]

Overall, we show that both proband and sister have a genotype that (1) is absent in hundreds of control subjects and in the unaffected parent (the father), (2) disrupts an important functional domain of the protein, and (3) disrupts the formation of gap junction channels. The data therefore support the notion of an association between the Cx40 mutation and the clinical phenotype and emphasize the importance of future studies to assess the possible involvement of Cx40 mutations as causative of the disease.

Acknowledgments

We thank Dr A.L. George for critical reading of the manuscript and Mss M. Fukuoka and C.R. Ingram for technical assistance.

Sources of Funding

This work was supported by research grant 21590921 (to Dr Makita), Scientific Research B (to Dr Mochizuki), and Grant-in-Aid for Scientific Research on Innovative Areas (HD Physiology) 22136007 (to Dr Makita) from the Ministry of Education, Culture, Sports, Science and Technology, Japan; a Health and Labor Sciences Research Grant for research on measures for intractable diseases from the Ministry of Health (2010-145) (to Dr Makita); the Mitsubishi Pharma Research Foundation (to Dr Makita); the Japan-France Integrated Action Program (SAKURA) (to Drs Makita and Schott); The Naito Foundation (to Drs Makita and Seki); the Support Center for Women Health Care Professionals and Researchers 21590921 (to Dr Seki); and grants GM057691, HL106632 and HL087226 from the National Institutes of Health (to Dr Delmar).

Disclosures

None.

References

1. Saffitz JE, Lerner DL, Yamada KA. Gap junction distribution and regulation in the heart. In: Zipes DP, Jalife J, eds. *Cardiac Electrophysiology: From Cell to Bedside.* Philadelphia, PA: Saunders; 2004:181–191.
2. Park DS, Fishman GI. The cardiac conduction system. *Circulation.* 2011; 123:904–915.
3. Ruan Y, Liu N, Priori SG. Sodium channel mutations and arrhythmias. *Nat Rev Cardiol.* 2009;6:337–348.
4. Firouzi M, Ramanna H, Kok B, Jongsma HJ, Koeleman BPC, Doevendans PA, Groenewegen WA, Hauer RNW. Association of human connexin40 gene polymorphisms with atrial vulnerability as a risk factor for idiopathic atrial fibrillation. *Circ Res.* 2004;95:e29–e33.
5. Gollob MH, Jones DL, Krahn AD, Danis L, Gong X-Q, Shao Q, Liu X, Veinot JP, Tang ASL, Stewart AFR, Tesson F, Klein GJ, Yee R, Skanes AC, Guiraudon GM, Ebihara L, Bai D. Somatic mutations in the connexin 40 gene (*GJA5*) in atrial fibrillation. *N Engl J Med.* 2006;354:2677–2688.

6. Lenègre J. Etiology and pathology of bilateral bundle branch block in relation to complete heart block. *Prog Cardiovasc Dis.* 1964;6:409–444.
7. Lev M, Kinare SG, Pick A. The pathogenesis of atrioventricular block in coronary disease. *Circulation.* 1970;42:409–425.
8. Probst V, Kyndt F, Potet F, Trochu JN, Mialet G, Demolombe S, Schott JJ, Baro I, Escande D, Le Marec H. Haploinsufficiency in combination with aging causes SCN5A-linked hereditary Lenègre disease. *J Am Coll Cardiol.* 2003;41:643–652.
9. Brink PA, Ferreira A, Moolman JC, Weymar HW, van der Merwe P-L, Corfield VA. Gene for progressive familial heart block type I maps to chromosome 19q13. *Circulation.* 1995;91:1633–1640.
10. de Meeus A, Stephan E, Debrus S, Jean M-K, Loiselet J, Weissenbach J, Demaille J, Bouvagnet P. An isolated cardiac conduction disease maps to chromosome 19q. *Circ Res.* 1995;77:735–740.
11. Kruse M, Schulze-Bahr E, Corfield V, Beckmann A, Stallmeyer B, Kurtbay G, Ohmert I, Schulze-Bahr E, Brink P, Pongs O. Impaired endocytosis of the ion channel TRPM4 is associated with human progressive familial heart block type I. *J Clin Invest.* 2009;119:2737–2744.
12. Royer A, van Veen TAB, Le Bouter S, Marionneau C, Griol-Charhbili V, Leoni A-L, Steenman M, van Rijen HVM, Demolombe S, Goddard CA, Richer C, Escoubet B, Jarry-Guichard T, Colledge WH, Gros D, de Bakker JMT, Grace AA, Escande D, Charpentier F. Mouse model of SCN5A-linked hereditary Lenègre's disease. Age-related conduction slowing and myocardial fibrosis. *Circulation.* 2005;111:1738–1746.
13. Schott JJ, Alshinawi C, Kyndt F, Probst V, Hoorntje TM, Hulsbeek M, Wilde AA, Escande D, Mannens MM, Le Marec H. Cardiac conduction defects associate with mutations in SCN5A. *Nat Genet.* 1999;23:20–21.
14. Watanabe H, Koopmann TT, Le Scouarnec S, Yang T, Ingram CR, Schott JJ, Demolombe S, Probst V, Anselme F, Escande D, Wiesfeld AC, Pfeufer A, Kaab S, Wichmann HE, Hasdemir C, Aizawa Y, Wilde AA, Roden DM, Bezzina CR. Sodium channel beta1 subunit mutations associated with Brugada syndrome and cardiac conduction disease in humans. *J Clin Invest.* 2008;118:2260–2268.
15. McNair WP, Ku L, Taylor MRG, Fain PR, Dao D, Wolfel E, Mestroni L; Familial Cardiomyopathy Registry Research Group. SCN5A mutation associated with dilated cardiomyopathy, conduction disorder, and arrhythmia. *Circulation.* 2004;110:2163–2167.
16. Miquerol L, Meysen S, Mangoni M, Bois P, van Rijen HVM, Abran P, Jongsma H, Nargeot J, Gros D. Architectural and functional asymmetry of the His-Purkinje system of the murine heart. *Cardiovasc Res.* 2004; 63:77–86.
17. Ackerman MJ, Priori SG, Willems S, Berul C, Brugada R, Calkins H, Camm AJ, Ellinor PT, Gollob M, Hamilton R, Hershberger RE, Judge DP, Le Marec H, McKenna WJ, Schulze-Bahr E, Semsarian C, Towbin JA, Watkins H, Wilde A, Wolpert C, Zipes DP. HRS/EHRA expert consensus statement on the state of genetic testing for the channelopathies and cardiomyopathies. *Heart Rhythm.* 2011;8:1308–1339.
18. Seki A, Coombs W, Taffet SM, Delmar M. Loss of electrical communication, but not plaque formation, after mutations in the cytoplasmic loop of connexin43. *Heart Rhythm.* 2004;1:227–233.
19. Anumonwo JMB, Taffet SM, Gu H, Chanson M, Moreno AP, Delmar M. The carboxyl terminal domain regulates the unitary conductance and voltage dependence of connexin40 gap junction channels. *Circ Res.* 2001;88:666–673.
20. Bochkov YA, Palmenberg AC. Translational efficiency of EMCV IRES in bicistronic vectors is dependent upon IRES sequence and gene location. *Biotechniques.* 2006;41:283–284.
21. Holm H, Gudbjartsson DF, Arnar DO, Thorleifsson G, Thorgeirsson G, Stefansdottir H, Gudjonsson SA, Jonasdottir A, Mathiesen EB, Njolstad I, Nyrnes A, Wilsgaard T, Hald EM, Hveem K, Stoltenberg C, Lochen M-L, Kong A, Thorsteinsdottir U, Stefansson K. Several common variants modulate heart rate, PR interval and QRS duration. *Nat Genet.* 2010;42:117–122.
22. Pfeufer A, van Noord C, Marciante KD, Arking DE, Larson MG, Smith AV, Tarasov KV, Muller M, Sotoodehnia N, Sinner MF, Verwoert GC, Li M, Kao WHL, Kottgen A, Coresh J, Bis JC, Psaty BM, Rice K, Rotter JI, Rivadeneira F, Hofman A, Kors JA, Stricker BHC, Uitterlinden AG, van Duijn CM, Beckmann BM, Sauter W, Gieger C, Lubitz SA, Newton-Cheh C, Wang TJ, Magnani JW, Schnabel RB, Chung MK, Barnard J, Smith JD, Van Wagoner DR, Vasan RS, Aspelund T, Eiriksdottir G, Harris TB, Launer LJ, Najjar SS, Lakatta E, Schlessinger D, Uda M, Abecasis GR, Muller-Myhsok B, Ehret GB, Boerwinkle E, Chakravarti A, Soliman EZ, Lunetta KL, Perz S, Wichmann HE, Meitinger T, Levy D, Gudnason V, Ellinor PT, Sanna S, Kaab S, Witteman JCM, Alonso A, Benjamin EJ, Heckbert SR. Genome-wide association study of PR interval. *Nat Genet.* 2010;42:153–159.
23. Thibodeau IL, Xu J, Li Q, Liu G, Lam K, Veinot JP, Birnie DH, Jones DL, Krahn AD, Lemery R, Nicholson BJ, Gollob MH. Paradigm of genetic mosaicism and lone atrial fibrillation: physiological characterization of a connexin 43-deletion mutant identified from atrial tissue. *Circulation.* 2010;122:236–244.
24. Sosinsky GE, Nicholson BJ. Structural organization of gap junction channels. *Biochim Biophys Acta.* 2005;1711:99–125.

CLINICAL PERSPECTIVE

Progressive familial heart block type I, also known as progressive cardiac conduction defect, is an inherited form of cardiac conduction system dysfunction that can lead to severe heart rhythm disturbances, including sudden cardiac death. The genetic causes of this disease are poorly understood. Here, we genetically screened 156 patients with progressive familial heart block type I. In addition to mutations in genes of the voltage-gated cardiac sodium channel complex (*SCN5A* and *SCN1B*), we found a novel germ line mutation in *GJA5*, the gene encoding the gap junction protein connexin40. The disease had an early onset and was associated with otherwise unexplained sudden cardiac death in the proband and his mother. The proband's sister is also affected. Cellular phenotype analysis revealed impaired gap junction formation at cell-cell interfaces and marked reduction of junctional conductance in cells expressing the mutated connexin40 protein. The results emphasize the importance of connexin40 in normal electrical propagation in the cardiac conduction system and open the possibility of including *GJA5* as a target gene for study in patients with progressive familial heart block type I.

Clinical and electrocardiographic characteristics of patients with short QT interval in a large hospital-based population

Akashi Miyamoto, MD, PhD,* Hideki Hayashi, MD, PhD,* Tomohide Yoshino, MD,* Tamiro Kawaguchi, MD,* Atsushi Taniguchi, MD,* Hideki Itoh, MD, PhD,* Yoshihisa Sugimoto, MD, PhD,* Makoto Itoh, MD, PhD,* Takeru Makiyama, MD, PhD,† Joel Q. Xue, PhD,‡ Yoshitaka Murakami, PhD,§ Minoru Horie, MD, PhD*

*From the *Department of Cardiovascular and Respiratory Medicine, Shiga University of Medical Science, Otsu, Shiga, Japan, †Department of Cardiovascular Medicine, Kyoto University Graduate School of Medicine, Kyoto, Kyoto, Japan, ‡General Electric Healthcare, Milwaukee, Wisconsin, §Department of Health Science, Shiga University of Medical Science, Otsu, Shiga, Japan.*

BACKGROUND Short QT syndrome is one of the underlying disorders associated with ventricular fibrillation. However, the precise prognostic implication of a short QT interval remains unclear.

OBJECTIVE The purpose of this study was to investigate the prevalence and long-term prognosis in patients with a shorter-than-normal QT interval in a large hospital-based population.

METHODS We chose patients with a short Bazett QTc interval from a database consisting of 114,334 patients to determine the clinical characteristics and prognostic value of a short QT interval.

RESULTS A total of 427 patients (mean age 43.4 ± 22.4 years) had a short QT interval with about a 1.2 times higher male predominance (234 men). The QTc interval was significantly longer in female than in male patients (363.8 ± 6.1 ms vs 357.1 ± 5.8 ms, $P < .0001$). The age-specific prevalence of patients with short QT interval was biphasic, peaking at young and old age. Atrial fibrillation and early repolarization were complicated with short QT interval in 39 (9.1%) and 26 (6.1%) patients, respectively. The prognosis of 327 patients (182 men; mean age, 46.4 ± 27.3 years) with a short QT interval could be assessed (mean follow-up period, 54.0 ± 62.0 months). During the follow-up, 2 patients, 1 of whom had early repolarization, developed life-threatening events, in contrast to 6 patients who died of noncardiac causes and did not have early repolarization.

CONCLUSION The prevalence of a short QT interval showed a slight male preponderance and biphasic age-dependent distribution in both genders. The complication rate of atrial fibrillation was higher in those with a short QT interval than in general populations. The long-term outcome suggested that early repolarization in a short QT interval might be associated with potential risk of lethal arrhythmia.

KEYWORDS Electrocardiography; QT interval; Prevalence; Prognosis; Repolarization

ABBREVIATIONS **AF** = atrial fibrillation; **CI** = confidence interval; **ECG** = electrocardiogram

(Heart Rhythm 2012;9:66–74)

Introduction

The QT interval is an invaluable prognostic marker for evaluating whether ventricular arrhythmia occurs.[1–3] Long QT syndrome is characterized by ventricular cells that fail to repolarize sufficiently quickly. On the other hand, short QT syndrome manifests an extremely abbreviated QT interval.[4,5] Genetic mutations underlie both syndromes, in which sudden cardiac death occurs.[6,7] It was reported that short QT syndrome complicated other electrocardiogram (ECG) abnormalities, such as atrial fibrillation (AF)[4] and early repolarization.[8] Although close attention must be paid to short QT interval, there may be overlap between normal QT interval and abnormally short QT interval.[9] In addition, the prognostic value of short QT syndrome in relation to AF or early repolarization is yet to be determined.

In our university hospital, more than 350,000 ECGs obtained from more than 110,000 patients are available for digital analysis. Using this large hospital-based population, we aimed: (1) to determine the distribution of the QT interval in the entire population, (2) to determine the clinical and ECG characteristics in individuals with short QT interval, and (3) to investigate the prognostic value of short QT interval.

Methods

The research protocol was approved by the Ethical Committee of Shiga University of Medical Science.

Address reprint requests and correspondence: Dr. Hideki Hayashi, Department of Cardiovascular and Respiratory Medicine, Shiga University of Medical Science, Otsu, Shiga 520-2192, Japan. E-mail address: hayashih@belle.shiga-med.ac.jp.

1547-5271/$ -see front matter doi:10.1016/j.hrthm.2011.08.016

Database

We analyzed resting 12-lead ECGs recorded in the university hospital of Shiga University of Medical Science. The 114,334 consecutive patients (55,091 female and 59,243 male patients) who had undergone ECG recordings between January 1983 and July 2010 were enrolled in the present study. A total number of 359,737 ECG recordings were obtained during this period. The 12-lead ECG was recorded for 10 seconds at a sweep speed of 25 mm/s, calibrated to 1 mV/cm in the standard leads. Twelve leads were simultaneously acquired. The ECG signals were recorded with a temporal sampling interval of 2 ms (i.e., 500 Hz). Digital data were stored in a server computer with 12-bit resolution.

Digital analysis of ECG

MUSE7.1 (GE Marquette Medical Systems, Inc., Milwaukee, Wisconsin) detected an identical P wave and QRS complex with a template matching technique. When AF (defined as irregular RR intervals with fibrillatory waves) was present, only QRS complex was identified by template-matching technique. ECG variables measured were composed by the averaged value during a 10-second recording time. QT interval was measured from the earliest detection of depolarization in any lead (QRS onset) to the latest detection of repolarization in any lead (T wave offset). T wave offset was determined by the time when 98% of the integrated area of T wave was over, which corresponded to a point where the T wave downsloping limb nearly joined the baseline. U wave was excluded. The QTc interval was calculated after correction for heart rate with the Bazett formula. Early repolarization was defined as an elevation at the junction between QRS complex and ST-segment ≥0.1 mV from baseline level in at least 2 leads. ST-segment elevation should be present in at least 2 consecutive beats to identify early repolarization. ECG recordings of a mean heart rate <50 or >100 beats/min were excluded from the analysis in the first analysis, and then the prevalence of short QT interval in patients with sinus bradycardia <50 beats/min was additionally investigated. ECGs with ventricular pacing were also excluded. Because all measurements of 12-lead ECG were digitally performed by virtue of software, neither intraobserver nor interobserver variability occurred in this study. To determine whether the automatic measure of QT interval correlates with the manual measure of QT interval, 1,000 ECGs were randomly selected, and then we compared the automatic and manual measure of the QT interval. The manual measure of the QT interval was performed by a standard tangential method in lead V5. The manual QT interval measurement was obtained by averaging the QT interval of 3 consecutive beats.

Data analysis

First, we constructed histograms according to QTc interval. QTc interval divided by 5 ms and the number of ECGs or patients used for frequency density were shown on the abscissa and the ordinate, respectively. Second, the prevalence of patients with a short QTc interval in association with age and gender was determined. Third, clinical and ECG characteristics of patients with a short QTc interval were determined. The prevalence of AF and early repolarization complicated by short QT interval was determined. Fourth, the prognostic value of a short QTc interval was assessed. Long-term outcome was determined by assessing whether sudden cardiac death, life-threatening ventricular arrhythmia, or any cause of death occurred. Patients were considered to have died suddenly if death was observed and had occurred within 1 hour after new or more serious complaints of probable cardiovascular cause. Life-threatening ventricular arrhythmia was determined by documented ECG. We reviewed the medical records of patients with short QT interval to evaluate their physical health status. In patients whose medical records were not available to determine prognosis, we gathered information on health status by a postal questionnaire. We performed gene analysis (see Supplementary Materials) in patients who developed life-threatening events with short QT interval.

Statistical analysis

The data are presented as mean ± SD. A comparison between 2 groups was performed with the Student t test or the nonparametric Mann-Whitney U test, as appropriate. Categorical variables were compared with χ^2 test. Kolmogorov-Smirnov test was performed to determine whether QTc interval distribution fit to a normal distribution. All tests were 2-tailed, and a value of $P < .05$ was considered statistically significant.

Results

In the database, there were 11,416 and 21,450 ECGs with heart rate of <50 and >100 beats/min, respectively. We excluded these ECGs from this study, thus 301,345 ECGs derived from 105,824 patients (56.0% men; mean age, 52.6 ± 20.7 years) were included for the analysis of this study. The autonomic QT interval measure was a little but significantly longer than the manual QT interval measure (421.8 ± 23.2 ms vs 418.0 ± 24.5 ms, $P < .0001$).

The mean difference between the manual and automatic QT interval measure was 3.8 ms (median 3.7 ms), and there was a significant linear correlation ($r = 0.95$, $P < .00001$) between the manual and autonomic measure of QT interval (Supplementary Figure 1), indicating the accuracy of the computer-assessed measure of QT interval.

Prevalence of QT interval

Figure 1 shows the distribution of the QTc intervals of total, male, and female patients. The histograms that were constructed as a function of the number of ECGs are shown in the upper row of Figure 1. The mean QTc interval was 421.4 ± 25.7 ms (95% confidence interval [CI] 382 to 482 ms, range 329 to 693 ms) in total patients; 418.9 ± 25.7 ms (95% CI 380 to 480 ms, range 331 to 693 ms) in male patients; and 424.7 ± 25.3 ms (95% CI 387 to 483 ms, range 329 to 687 ms) in female patients. The QTc interval was significantly ($P < .0001$) longer in female patients than

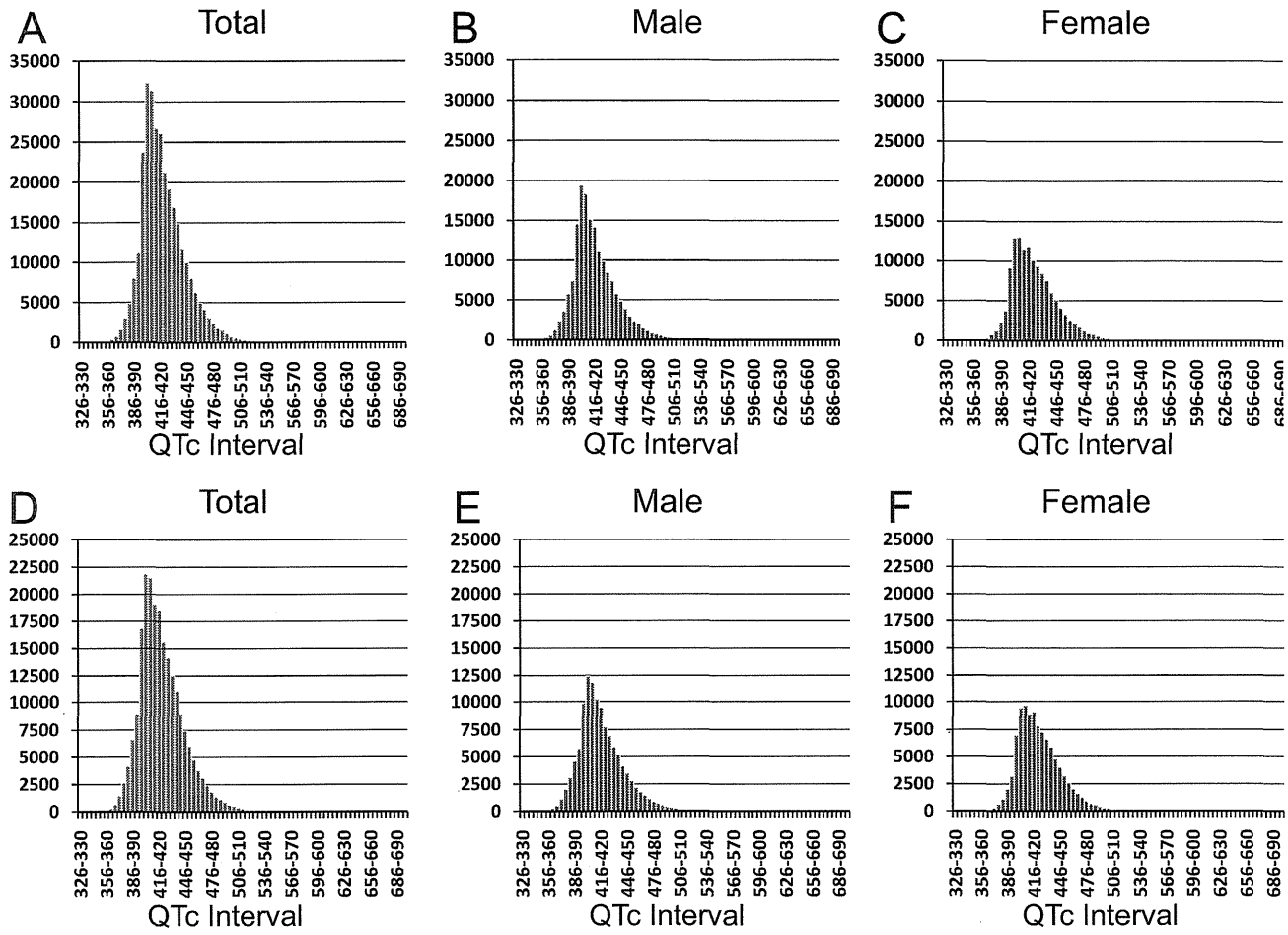

Figure 1 Distribution of Bazett QTc interval according to the number of patients (upper row) and the number of ECGs (lower row). Histograms of total, male, and female patients in this study population are displayed in panels A and D, B and E, and C and F, respectively.

in male patients. The QTc interval distributions did not fit a normal distribution curve ($P < .01$ for each) because the distributions were asymmetrical and right skewed. The histograms of QTc interval that were generated as a function of the number of patients are shown in the lower row of Figure 1. Similarly, the histograms of the QTc interval were right-skewed, which failed to fit to a normal distribution ($P < .01$ for each). The mode of QTc interval was 401 to 405 ms (range 329 to 693 ms), 401 to 405 ms (range 331 to 693 ms), and 406 to 410 ms (range 329 to 687 ms) in total, male, and female patients, respectively. Table 1 shows the lowest percentiles of QTc interval. The QTc interval at the lowest 2.5 percentile was longer than the lower limit of normal QTc interval previously reported.[9] The QTc interval[10,11] at the lowest 0.15 percentile was similar to the lower border of QTc interval. We therefore adopted a definition of short QT on the basis of previous studies, the cutoff value matching the 0.15 percentile of our whole population (234 male patients with QTc interval ≤362 ms, 193 female patients with QTc interval ≤369 ms). Furthermore, we divided the short QT population into percentiles and selected the 2.5 percentile of the short QT population as the very short QT (Table 2).

Clinical characteristics of short QT interval

Four hundred twenty-seven patients with short QT interval were chosen for the analysis according to the abovementioned rationale. The prevalence of patients with a short QT interval was about 1.2 times higher in male patients (N = 234) than in female patients (N = 193). The mean age was not different between male and female patients (41.9 ± 21.5 years vs 45.2 ± 23.4 years). Table 3 shows clinical characteristics of the patients with short and very short QTc intervals. The mean age was not different between short and

Table 1 The lowest percentiles of Bazett QTc interval for this study population

	Bazett QTc interval (ms)	
Percentile	Male	Female
2.5	380.0	387.0
2.0	378.0	386.0
1.0	373.0	381.0
0.5	369.0	376.0
0.15	362.0	369.0
0.1	361.0	367.0
0.0	331.0	329.0